HES1 and *ID3* temporally regulate p27 levels and endothelial cell flow-mediated quiescence depth

Natalie T Tanke[a], Ziqing Liu[b], Tianji Yu[b], Morgan Oatley[b], Pauline Bougaran[b], Kaitlyn Quigley[b], Jeanette Gowen Cook[c], and Victoria L Bautch[a,b,d,#]

[a]Curriculum in Cell Biology and Physiology, The University of North Carolina at Chapel Hill, Chapel Hill, North Carolina 27599, USA
[b]Department of Biology, The University of North Carolina at Chapel Hill, Chapel Hill, North Carolina 27599, USA
[c]Department of Biochemistry and Biophysics, The University of North Carolina at Chapel Hill, Chapel Hill, North Carolina 27599, USA
[d]McAllister Heart Institute, The University of North Carolina at Chapel Hill, Chapel Hill, North Carolina 27599, USA

[#]Corresponding author: Victoria L Bautch, PhD
Professor of Biology
Department of Biology, CB#3280
University of North Carolina at Chapel Hill
Chapel Hill, NC 27599 USA
Email: bautch@med.unc.edu

Running head: Endothelial cell quiescence depth varies with time

Words: 8,293 (main text and references)
Abstract: 197 words
Figures: 6
Supplemental Figures: 6
Supplemental Tables: 6
References: 68

Keywords: Endothelial cell, laminar shear stress, quiescence depth, p27, cell cycle, *HES1*, *ID3*

GRAPHICAL ABSTRACT

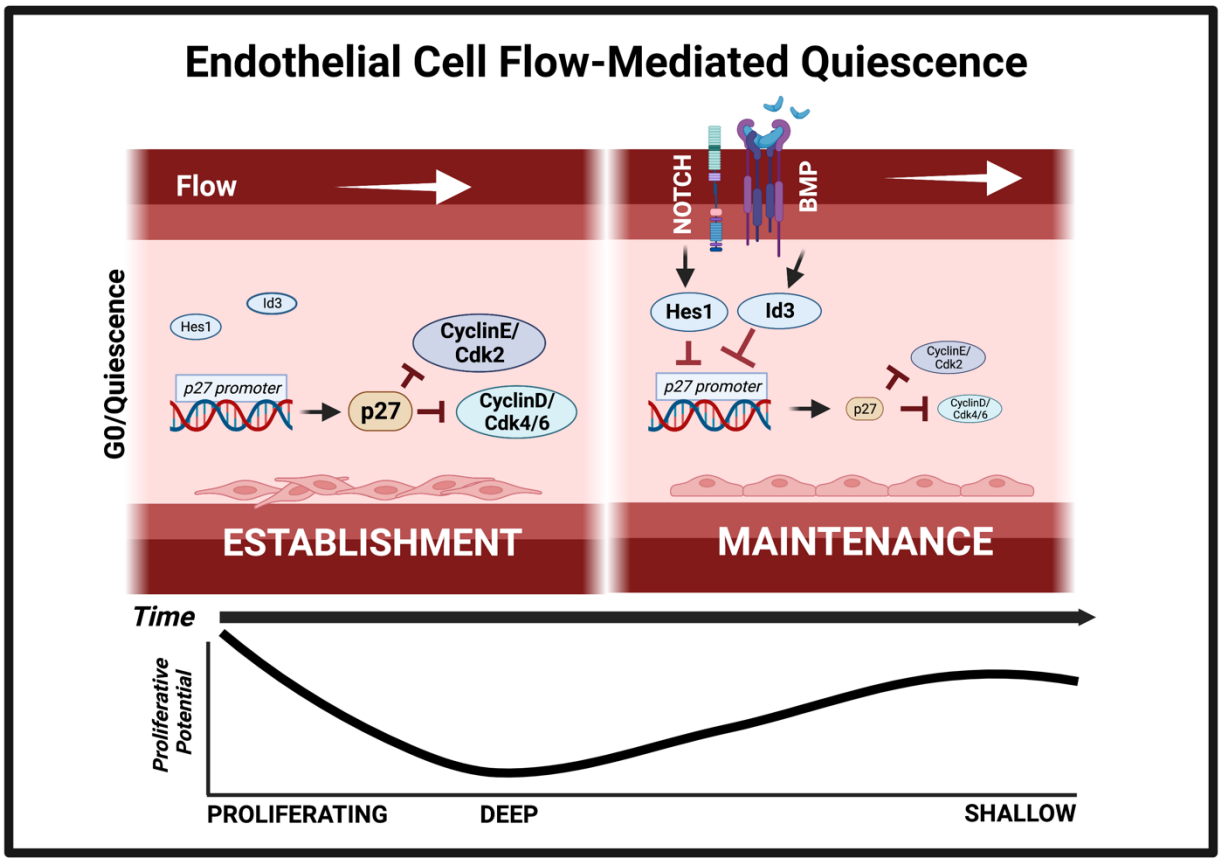

HIGHLIGHTS

- Different quiescence stimuli lead to distinct transcriptional and functional quiescence profiles in endothelial cells
- Flow-mediated endothelial quiescence depth changes from deep to shallow over time and correlates with p27 levels
- *HES1* and *ID3*, flow-upregulated repressors of p27 expression, are required for the temporal shift in quiescence depth under flow

ABSTRACT

Vascular endothelial cells regulate their cell cycle as blood vessels remodel and mature, and as they transition from active angiogenesis to quiescence. Mechanical cues provided by fluid shear stress orchestrate this transition, and laminar blood flow instigates a quiescent (G_0) state and homeostasis. However, how flow-mediated quiescence is set up and maintained is poorly understood. We found that flow-mediated endothelial cell quiescence has unique properties and temporal regulation of quiescence depth. Flow-exposed endothelial cells had a distinct transcriptome, and quiescent endothelial cells re-entered the cell cycle more rapidly after extended flow exposure compared to contact inhibition, indicating a shallow quiescence depth. The cell cycle inhibitor *CDKN1B* (p27) was required for endothelial cell flow-mediated quiescence but was not significantly expressed after extended flow exposure. Rather, flow-exposed endothelial cells first established a deep quiescence that subsequently became shallow, and p27 levels positively correlated with these distinct quiescent states. *HES1* and *ID3*, transcriptional repressors of p27 downstream of flow-regulated Notch and BMP signaling, were required for flow-mediated quiescence depth changes and the reduced p27 levels associated with shallow quiescence. These findings are consistent with a model whereby flow-mediated endothelial cell quiescence depth is temporally regulated downstream of transcriptional regulation of p27.

107 **INTRODUCTION**
108

109 Blood vessel network expansion via sprouting angiogenesis during development
110 is followed by vascular homeostasis; this transition depends on the appropriate
111 responses of endothelial cells to incoming signals, including laminar shear stress
112 provided by blood flow. Laminar flow leads to endothelial cell cytoskeletal realignment
113 and polarization relative to the flow vector and dramatically reduces proliferation [1–6].
114 Transcriptional profiles reveal numerous changes with flow exposure [7,8], and signaling
115 pathways such as Notch and BMP are upregulated to promote alignment and vascular
116 homeostasis [9,10]. Once vascular homeostasis is achieved, endothelial cells rarely divide
117 [7,11,12]; rather, they are arrested in a quiescent (G_0) state but capable of re-entering the
118 cell cycle when stimulated by angiogenic growth factors such as VEGF-A [13–15]. How
119 flow-mediated vascular quiescence is established and maintained is poorly understood,
120 yet it is critical to blood vessel function.
121

122 In non-endothelial cells, quiescence is influenced by cell type and the quiescence
123 stimulus, and its establishment and maintenance has been extensively studied in
124 fibroblasts and transformed cells [16–18]. Quiescence stimuli include growth factor
125 deprivation, contact inhibition, loss of cell adhesion or cell cycle inhibition. Different
126 quiescence stimuli applied to the same cells lead to transcriptional profiles that are
127 partially overlapping but have strong unique signatures, suggesting that the quiescence
128 stimulus qualitatively influences the transcriptome at steady state [16,17]; however, how
129 these differences affect quiescence properties is poorly understood.

130 The cell cycle is regulated by cyclins and cyclin-dependent kinases (CDKs) that
131 promote and CDK inhibitors that block cell cycle progression [19]. In cycling cells, proteins
132 are post-translationally modified and/or carry destabilization sequences that lead to
133 rapid gain and loss of function required for passage through the cell cycle [20,21]. In
134 contrast, quiescence is characterized by transcriptional repression of cell cycle
135 activators and often by upregulation of cell cycle inhibitors [16,19]. Thus, upon removal of a
136 quiescence stimulus cell cycle re-entry is delayed, and re-entry time is an indicator of
137 quiescence depth [22,23]. Quiescence depth is variable; for example, quiescent fibroblasts
138 have delayed cell cycle re-entry that positively correlates with temporal exposure to the
139 quiescence stimulus [22,23]. Non-homogeneous quiescence depth is also documented in
140 muscle stem cells that respond to injury-induced circulating cues by entering a shallow
141 quiescence called "G_0 alert" that allows for prompt proliferation in response to a
142 subsequent injury [24]**.** Moreover, spontaneous quiescence has been described recently,
143 whereby epithelial cells enter quiescence in the absence of obvious environmental or
144 pharmacological cues, suggesting that quiescence entry has a stochastic component
145 and/or complex inputs [17,25]. Thus, how quiescence is established, maintained, and
146 exited is complex.
147
148 We examined properties of flow-induced endothelial cell quiescence, and found
149 that laminar flow-induced endothelial cell quiescence is transcriptionally distinct from
150 contact-mediated quiescence and functionally exhibits dynamic temporal regulation of
151 quiescence depth. Prolonged laminar flow leads to an initial stage of deep quiescence
152 followed by transition to a shallow quiescence depth. Temporal changes in endothelial

153 cell quiescence depth positively correlate with expression of the cell cycle inhibitor p27.
154 p27 repression and the shift from deep to shallow quiescence depth requires the
155 transcription factors *HES1* and *ID3*, targets of the Notch and BMP signaling pathways,
156 respectively, that are up-regulated by laminar flow and repress p27 levels. These
157 findings show that endothelial cells respond to laminar flow-mediated quiescence
158 signals dynamically in a way that correlates with flow-mediated transcriptional changes
159 affecting p27 expression, and suggest complex regulation of quiescence depth that may
160 protect from senescence and facilitate the robust angiogenic response required in
161 physiological settings such as wound healing.
162

163 **MATERIALS AND METHODS**

164

165 ***Cell culture***

166 HUVEC (Lonza #C2519A) were cultured according to the manufacturer's
167 recommendations in EBM2 (CC-3162, Lonza) supplemented with added growth factors
168 (Bullet kit, CC-3162, Lonza, referred to as EGM2) at 37°C and 5% CO_2 and used
169 between passages 2-4, unless otherwise noted. Critical experiments were replicated
170 with multiple lots of HUVEC.

171

172 ***Microscopy***

173 Imaging was performed using confocal microscopy (Olympus Fluoview FV3000,
174 IX83) using 405nm, 488nm, 561nm, and 640nm lasers and a UPlanSApo 40x silicone-
175 immersion objective (NA 1.25), UPlanSApo 60x oil-immersion objective (NA 1.40), or
176 UPlanSApo 100x oil-immersion objective (NA 1.40). Imaging was performed at RT and
177 images were acquired with the Fluoview FV31S-SW software. All imaging analysis was
178 completed in FIJI [26]. For each replicate within an experiment, images were acquired at
179 the same settings.

180

181 ***Immunofluorescence***

182 Endothelial cells were fixed in 4% PFA (15713 (100504-940), VWR) at 37°C for
183 10 min and permeabilized in 0.1% Triton (T8787-100ML, Sigma) in PBS for 10 min at
184 RT. Following permeabilization, HUVEC were blocked for 1 hr at RT in 5% NBCS
185 (Gibco, #16010-159), antibiotic-antimycotic (Gibco, #15240062), 0.1% sodium azide
186 (Sigma s2002-100G). Following 3X washes in PBS, cells were incubated in primary

187 antibody diluted in blocking solution and incubated for 24 hr at 4°C (**Supp. Table S2**,
188 primary antibody information). Cells were washed 3X with PBS before adding
189 secondary antibody diluted in blocking solution and incubated for 3 hr at RT in the dark
190 (**Supp. Table S3**, secondary antibody information). Slides were mounted with coverslips
191 using Prolong Diamond Antifade mounting media (P36961, Life Technology), sealed
192 with nail polish, and stored at 4°C. Glass-bottom Ibidi slides or well dishes were stored
193 in 1X PBS to prevent desiccation.
194
195 ***Endothelial Cell Transfection***
196 HUVEC were grown to subconfluency and treated with siRNAs **(Supp. Table S4,**
197 siRNA information**)** diluted in OptiMem (Gibco, #11058021) and Lipofectamine 3000
198 (ThermoFisher, #L3000015) according to manufacturer's protocol
199 (https://www.thermofisher.com/us/en/home/references/protocols/cell-
200 culture/transfection-protocol/lipofectamine-2000.html). Briefly, siRNA at 0.48 μM in Opti-
201 MEM (31985-070, Gibco) and a 1:20 dilution of Lipofectamine in Opti-MEM were
202 incubated separately at RT for 5 min, then combined and incubated at RT for 15 min.
203 HUVEC were transfected at 80% confluency with siRNA at 37°C for 24 hr. After 24 hr,
204 media was replaced with 10 mL of fresh EGM-2. All experiments were initiated 48 hr
205 following exposure to siRNA.
206
207 ***Endothelial Cell Flow and Quiescence Depth***
208 Endothelial cells were exposed to laminar flow for 72 hr at 15dyn/cm^2 using an
209 Ibidi pump system (CC-1090, Ibidi). Static (non-flow) control slides were seeded at

210 lower densities and incubated for 48 hr prior to fixation with 4% PFA, and subconfluence
211 status was verified visually prior to fixation and collection. All HUVEC for flow
212 experiments were cultured in EBM2 supplemented with 2% FBS, 1% antibiotic-
213 antimycotic (Gibco, #15240062), and 1% Nystatin (Sigma, #N1638-20ML). To prevent
214 cell shearing, cells were first exposed to 5 d/cm^2 flow for 30 min, 10 d/cm^2 for 30 min,
215 and then 15 d/cm^2 for the remaining 16 hr (flow establishment (Flow-E)) or 72 hr (flow
216 maintenance (Flow-M)). For orbital flow experiments, an orbital shaker (Hoefer Red
217 Rotor Mixer Platform Shaker PR70-115V) was used as previously described [27].
218
219 Flow-mediated quiescence depth experiments were performed as follows. After
220 16 or 72 hr of exposure to laminar flow, cells were pulse labeled for 30 min with EdU
221 and either fixed (0 hr) or fixed 2, 5, or 8 hr post-flow in 4% PFA for 10 min at RT, then
222 visualized for EdU and/or stained for antibodies as described (**Supp. Tables S2, S3**).
223
224 ***Contact Inhibition and Quiescence Depth***
225 Endothelial cells were seeded in a 6-well plate at 1.2 million cells/well (high
226 density) or at 200,000 cells/well (low density) and incubated for 24 hr. A p1000 pipette
227 tip was used to scrape the cell monolayer and create a gap as previously described [28].
228 Following the scratch, cells were pulse labeled with EdU for 30 min and fixed (0 hr) or
229 fixed 2, 5, or 8 hr post-scratching in 4% PFA for 10 min at RT, then visualized for EdU
230 and/or stained for antibodies as described (**Supp. Table S2, S3**). Cells within 1000 μm
231 of the scratch edge were imaged **(Supp. Fig. 2a**).
232

233 ***EdU Labeling***

234 EdU labeling was performed according to the Click-IT EdU 488, 594, or 647
235 protocol (Invitrogen, C10337). For all experiments with the exception of quiescence
236 depth experiments, cells were incubated in EdU for 1 hr at 37°C in 5% CO_2 and fixed
237 with 4% PFA for 10 min at RT. For quiescence depth experiments, cells were incubated
238 in EdU for 30 min at 37°C in 5% CO_2 and fixed at 4% PFA for 10 min at RT.

239

240 ***Quantification of Positive Endothelial Cells***

241 The DAPI channel was used as a nuclear mask, and nuclear fluorescence
242 intensity was measured for each cell per image field. Positive cells were defined as
243 those above the sensitivity threshold. For each image acquired, the percentage of
244 positive cells was quantified.

245

246 ***Quantification of Cell Axis Ratio***

247 Cell shape and alignment were measured as described previously [7]. Cells were
248 stained for VE-cadherin upon fixation, and measured at the longest axis of cell divided
249 by shortest axis to calculate the cell axis ratio, with the longest cell axis being the
250 direction of flow.

251

252 ***Western Blot Analysis***

253 Western blot analysis was performed according to [29] with modifications. Briefly,
254 cells were scraped into PBS, centrifuged at 13000 rpm at 4°C for 20 min, then
255 resuspended in RIPA buffer with protease/phosphatase inhibitor (5872S, Cell

256 Signaling). The cell pellet was resuspended in sample loading buffer and dithiothreitol
257 (R0861, Thermo Fisher) and boiled for 10 min. 10µg of sample was run on a 10% SDS-
258 PAGE gel (161-0183, BioRad) then transferred onto a membrane for 1.5 hr on ice.
259 Membranes were incubated in primary antibodies overnight at 4°C (**Supp. Table S2**).
260 Membranes were washed 3X in PBST and stained with secondary antibody diluted in
261 One-Block at RT for 1 hr (**Supp. Table S3**). Immobilon Forte HRP Substrate
262 (WBLUF0100, 769 Millipore Sigma) was added for 30 sec. Blots were exposed for 2 sec
263 ChemiDoc XRS with Chemi High Resolution setting.
264

265 ***RT-qPCR***

266 RNA was extracted using TRIzol (15596018, Invitrogen). cDNA was generated
267 from 1ug RNA using iScript reverse transcription kit (Bio-Rad, #1708891) and diluted
268 1:3 in water. qRT–PCR was performed using iTaq Universal SYBR Green SuperMix
269 (Bio-Rad, #1725121). SYBR Green real-time PCR was performed in triplicate on the
270 Applied Biosystems QuantStudio 6 Flex Real-Time PCR System (**Supp. Table S5**). For
271 quantification, relative expression of each gene to β-actin in each sample was
272 calculated by 2^(CT of gene−CT of β-actin). Statistical significance was determined by
273 unpaired Student's T-test.
274

275 ***Bulk RNA Sequencing and Analysis***

276 RNA was extracted using TRIzol (15596018, Invitrogen). For each condition 3
277 Ibidi slides were pooled. Stranded libraries were prepared using KAPA mRNA
278 HyperPrep Kit (7961901001, Roche) and sequenced using NovaSeq S1 at the UNC

279 Sequencing Core. Data was analyzed as described previously [30]. Briefly, 2–3×10^7 50 bp
280 paired-end reads per sample were obtained and mapped to the human genome
281 GRCh38 with STAR using default settings [31]. Quality of sequencing reads was
282 confirmed with FastQC before mapping. Mapping rate was over 87% for all samples
283 (**Supp. Table S6**), and gene expression was determined with Htseq-count using the
284 union mode [32]. Genes with low expression were filtered out (total raw counts in all
285 samples < 10), differential expression analysis was performed with DESeq2 [33] using
286 default settings in R, and lists of differentially expressed genes were obtained (p
287 adjusted <0.1). Gene ontology analysis was performed using enrichGO function in the R
288 package clusterProfiler. All gene ontology terms shown in this study have a corrected P
289 value < 0.1.
290
291 ***Quiescence Score***
292 The endothelial quiescence score was calculated using the following formula: QS
293 = 1/n$\sum_{i=1}^{n} QSUi$-1/m$\sum_{j=1}^{m} QSDj$ (QS = Quiescence Score, QSU = QS of upregulated
294 genes under quiescence (total n genes), QSD = QS of downregulated genes under
295 quiescence (total m genes)). Selected genes were upregulated or downregulated
296 relative to control, in this case static (non-flow) samples. All genes were normalized for
297 sequencing depth and scaled for expression as previously described [8]. To generate the
298 gene list used for the endothelial quiescence score we utilized two datasets (**Supp.
299 Table S1**). First, S/G_2/M phase associated genes from the CellCycleScoring function of
300 the R package Seurat were tested in our scRNAseq HUVEC dataset
301 (https://satijalab.org/seurat/articles/cell_cycle_vignette.html). Genes that were down-

302 regulated under flow were included in the score. Second, genes that were consistently
303 upregulated in response to different quiescence stimuli in non-endothelial cells in a
304 previous report were tested in our scRNA dataset, and if upregulated in response to
305 flow they were included [16]. The scRNAseq HUVEC dataset was previously published
306 and is available in NCBI GEO database (accession code GSE151867[8]). The epithelial
307 quiescence score was developed by the Barr lab as previously described, and utilized
308 an independent gene list generated using non-transformed human epithelial cell
309 data[17,34].
310
311 ***Mouse scRNAseq data***
312 scRNAseq data of aged mouse (the *Tabula Muris Senis* dataset) was
313 downloaded from figshare (https://doi.org/10.6084/m9.figshare.8273102.v2) and
314 analyzed using Seurat [35]. Endothelial cells were extracted from the original gene count
315 matrix and down sampled for the 1-, 3- and 18-month time points. Endothelial cells
316 below the sensitivity level for *Cdkn1b* expression were excluded from analysis.
317
318 For mouse ear scRNAseq, a previously generated dataset (Liu et al, in
319 preparation) using enriched endothelial cells from the ear at P8 (postnatal day 8) or
320 adult (2-2.5 months) was analyzed. A total of ten vascular endothelial cell populations
321 were identified by dimension reduction and clustering analysis with Seurat. The
322 percentage of *Cdkn1b-expressing* cells in the endothelial cells of 9 of the 10
323 subpopulations (2 samples for each stage) was calculated (one subpopulation had < 10
324 cells in adult stage and was excluded from analysis).

325 ***Statistics***

326 Unpaired Students T-Test was used to determine statistical significance in
327 situations with two experimental groups, and One-Way ANOVA with Tukey correction
328 was used for experimental groups of 3 or more. All statistical tests and graphs were
329 made using the Prism 9.4.1 software (GraphPad Software). *$*p \leq 0.05$, ** $p \leq 0.01$, *** p
330 ≤ 0.001, ****$p \leq 0.0001$, ns = not significant*. Statistical methods and significance
331 parameters are also described in the Figure Legends.

332

333 ***Data availability***

334 Bulk RNA Sequencing data has been deposited in GEO under accession code
335 GSE213323. Data available upon request.

336

337

338

339

340 **RESULTS**
341
342 **Laminar flow-exposed endothelial cells have a distinct transcriptional profile**

343 Endothelial cells exposed to laminar shear stress align relative to the flow vector
344 and significantly reduce their proliferation rate, hallmarks of vascular homeostasis or
345 quiescence [1,2,5]. To determine whether endothelial cells exposed to laminar flow were
346 transcriptionally quiescent relative to proliferating cells (static, non-flow), we first applied
347 a published quiescence score generated in non-endothelial epithelial cells [34] to a
348 scRNAseq dataset that we previously generated in primary endothelial cells (HUVEC,
349 human umbilical vein endothelial cells) exposed to laminar flow [8]. Application of the
350 epithelial quiescence score to this data binned by flow status showed that endothelial
351 cells exposed to homeostatic laminar flow (here called Flow-Maintenance (15d/cm^2, 72
352 hr)) had a significantly higher score than non-flowed (static condition, 48hr post-seeding
353 and subconfluent) control endothelial cells **(Fig 1a)**. Previous UMAP analysis of this
354 dataset revealed 9 groups that primarily separated by flow condition, and the cluster
355 containing the majority of cells exposed to flow (Flow Cluster 1) had a significantly
356 higher epithelial quiescence score compared to the equivalent cluster in the static group
357 (Static Cluster 1), indicating that this published quiescence score positively correlates
358 with flow-exposed endothelial cells that are predicted to be quiescent. Quiescence
359 score comparisons among other flow clusters with fewer cells showed heterogeneity
360 relative to Flow Cluster 1, and a similar comparison of static clusters also revealed
361 heterogeneity relative to Static Cluster 1, indicating that these distinct clusters exhibit
362 quiescence heterogeneity. This trend was especially noted for Flow Cluster 2, Static
363 Cluster 2, and Mix Cluster (contains endothelial cells from both flow and static

364 conditions) that were previously defined as proliferative populations and had a
365 significantly reduced quiescence score **(Fig. 1a)**[8].
366
367 We next used the same dataset to generate an independent endothelial
368 quiescence score. Since a hallmark of cellular quiescence is downregulation of
369 proliferation markers and upregulation of cell cycle inhibitors [16], this score was primarily
370 generated using expression levels of cell cycle genes that were up- or downregulated in
371 endothelial cells exposed to extended laminar flow (Flow Maintenance (Flow-M),
372 15dyn/cm^2/72hr) (**Supp. Table 1**). The endothelial quiescence score was then applied
373 to the dataset to verify that the score predicted the relationships. Consistent with the
374 epithelial score, flow cluster 1 had a significantly higher quiescence score compared to
375 static cluster 1, and the clusters associated with proliferation had significantly lower
376 scores (**Fig. 1b**)**.** These findings indicate that endothelial cells exposed to homeostatic
377 laminar flow (Flow-M) are in a transcriptionally quiescent cell cycle state.
378
379 We next applied the endothelial quiescence score to an independently generated
380 dataset to validate the score and further examine endothelial cell quiescence
381 relationships. Both fibroblasts and epithelial cells exposed to different quiescence
382 stimuli have unique transcriptional profiles [16,17], so we asked whether the mode of
383 quiescence induction affected the quiescence score of endothelial cells exposed to
384 static vs. extended laminar flow (Flow-M) or low vs. high density static (non-flow)
385 conditions. Application of the endothelial quiescence score to HUVEC bulk RNA seq
386 data showed significant increases under flow and high density compared to static and

387 low density conditions, respectively **(Fig. 1c)**, and these relationships held when the
388 epithelial quiescence score was applied in the same manner **(Supp. Fig. 1a)**. Venn
389 diagrams revealed that extended laminar flow and contact inhibition have both shared
390 and distinct transcriptional changes in endothelial cells, with approximately one quarter
391 of the regulated genes shared for up- and down-regulated categories (upregulated:
392 21.7% (494/2272) flow and 24.3% (494/2030) density shared genes; down-regulated
393 25.1% (573/2282) flow and 23.7% (573/2415) density shared genes) (**Supp. Fig. 1b**).
394 Further analysis of highly differentially expressed genes revealed only one overlapping
395 gene (*CCDC190*) that was downregulated between flow and high density conditions,
396 and no genes were highly upregulated with both flow and high density conditions,
397 suggesting that while there is some overall overlap, the quiescence profiles of
398 endothelial cells exposed to extended laminar flow or high density are largely distinct
399 **(Supp. Fig. 1c-f)**. Gene Ontogeny (GO) analysis revealed several terms linked to
400 migration and development shared by endothelial cells under extended laminar flow and
401 high density (**Supp. Fig. 1g-j**). Although endothelial cell quiescence is sometimes
402 characterized as an inactive state, migration of quiescent cells has been documented[36]
403 and contributes to developmental and pathological angiogenesis [37–39]. However, more
404 prominent were numerous categories unique to either flow exposed or high density
405 endothelial cells; for example, flow exposed cells had adhesion terms upregulated and
406 protein ubiquitination terms downregulated, while contact inhibited endothelial cells had
407 TGF-β signaling upregulated and mitochondrial gene expression downregulated (**Supp.
408 Fig. 1g-j**), consistent with the largely unique transcriptional profiles for different modes
409 of endothelial cell quiescence.

410 We next examined how expression of specific cell cycle regulatory genes varied
411 under extended flow exposure or high density, and found that expression of cell cycle
412 activators was down-regulated regardless of quiescence induction stimulus, while
413 transcription of cell cycle inhibitors showed an expected increased trend under high
414 density conditions but not under flow exposure **(Fig. 1d-e).** Thus, endothelial cells
415 respond to extended laminar flow exposure with a distinct quiescence transcriptional
416 profile compared to high density-induced quiescence that includes differences in how
417 cell cycle inhibitors are regulated, suggesting unique properties of flow-mediated
418 endothelial cell quiescence.
419

420 **Shallow quiescence depth characterizes endothelial cells exposed to extended**
421 **laminar flow**

422 Quiescence depth varies in fibroblasts and stem cells, as defined by the time to
423 re-enter the cell cycle upon removal of the quiescence stimulus [22–24]. The lack of cell
424 cycle inhibitor RNA upregulation in endothelial cells exposed to laminar flow led us to
425 hypothesize that laminar flow-exposed cells are in a relatively shallow quiescence state.
426 To measure endothelial cell quiescence depth, we assessed cell cycle re-entry time via
427 EdU pulse labeling and pRB (phospho-retinoblastoma protein) expression at defined
428 times after removal of the quiescence stimulus (**Supp. Fig. 2a**) [40,41]. The timepoints for
429 analysis were selected based on the doubling time of HUVEC (Lonza Manufacturer).
430 EdU labels cells in S-phase, and phosphorylation releases RB from E2F transcription
431 factors, allowing for progression through the G_1-S checkpoint and proliferation [41,42].
432 Endothelial cells exposed to either extended laminar flow (Flow-M) or contact inhibition

433 had significantly reduced percentages of EdU-labeled **(Fig. 2a-b, d-e)** and pRB positive
434 cells **(Fig. 2a, c, d, f)** at the end of the flow or contact inhibition period, consistent with
435 previously published work [7,12,43], as well as decreased pRB nuclear intensity **(Supp.**
436 **Fig. 2b-c).** Endothelial cells released from extended laminar (Flow-M) significantly
437 increased EdU-labeled and pRB positive cells within 2 hr of flow cessation, while
438 endothelial cells released from contact inhibition did not show significant increases in
439 EdU-labeling and pRB reactivity until 8 hr post-release **(Fig. 2a-f, Supp. Fig. 2b-c).**
440 These findings show that endothelial cells exposed to homeostatic laminar flow (Flow-
441 M) are less deeply quiescent compared to endothelial cells that are contact inhibited.
442

443 **Cell cycle inhibitor p27 expression correlates with quiescence depth and is**
444 **required for flow-mediated quiescence**

445 Although several cell cycle inhibitors participate in cell cycle progression, p27
446 (*CDKN1B*) is often upregulated with quiescence in non-endothelial cells [44–46]. However,
447 after exposure to extended laminar flow (Flow-M), RT-qPCR analysis revealed a
448 significant decrease in *CDKN1B* RNA expression, and protein analysis showed a highly
449 significant decrease in the percentage of p27+ endothelial cells relative to static controls
450 (static 47% vs. flow 2%) **(Fig. 3a-c; Supp. Fig 3a,c)**. In contrast, p27 protein levels
451 increase in contact inhibited endothelial cells [43], and we confirmed that both RNA levels
452 and the percentage of p27+ endothelial cells significantly increased with contact
453 inhibition compared to low density controls (14% low vs. 99% high density) **(Fig. 3d-f;**
454 **Supp. Fig. 3b-c).** It is striking that endothelial cells exposed to extended laminar flow
455 (Flow-M) and with shallow quiescence depth have 2% p27+ cells, while contact inhibited

456 endothelial cells with more profound quiescence depth have 99% p27+ cells. Taken
457 together, these findings show that p27 expression positively correlates with quiescence
458 depth in endothelial cells.
459
460
461 We next asked whether p27 is functionally required for flow-mediated quiescence
462 induction in endothelial cells by depleting p27 via siRNA knockdown (KD). p27-depleted
463 cells exposed to extended flow (Flow-M) had a significantly increased percentage of
464 cells positive for EdU-labeling and staining for Ki67, a marker of cells in S, G_2, or M
465 phase [47], compared to non-targeting (NT) siRNA controls (**Fig. 4a-b; Supp. Fig. 3d-f**),
466 indicating that, despite relatively low expression at the end of flow exposure, p27 is
467 required for flow-mediated endothelial cell quiescence.
468
469 To better understand how p27 affects endothelial cell quiescence, we
470 transcriptionally profiled quiescent endothelial cells depleted for p27 under extended
471 laminar flow and high density conditions. Consistent with differences in p27 expression
472 with different quiescence stimuli, there was little overlap in the profiles of genes up- or
473 down-regulated in each condition upon p27 depletion (upregulated: 9.0% (12/133) flow
474 and 8.6% (12/139) density shared genes; down-regulated 13.4% (18/134) flow and
475 0.4% (18/313) density shared genes) **(Supp. Fig. 4a)**. Further analysis of highly
476 differentially expressed genes revealed no overlapping genes between control and p27
477 depleted cells under extended laminar flow or contact inhibition, and comparison of
478 gene ontology (GO) terms of p27 depleted cells to controls under extended laminar flow
479 or contact inhibition revealed no shared terms **(Supp. Fig. 4b-i)**, suggesting that p27

480 affects endothelial cell transcriptional quiescence programs differently depending on the
481 quiescence stimulus.
482
483 **Flow-mediated quiescence depth is temporally regulated in endothelial cells**
484 p27 is functionally required to mediate flow-mediated endothelial cell repression
485 of proliferation despite having significantly reduced expression by 72 hr of laminar flow
486 exposure (Flow-M). We hypothesized that p27 expression levels fluctuated during the
487 flow period, and temporal analysis showed that the percentage of p27+ cells
488 significantly increased 16 hr after flow initiation compared to the 0 hr levels (time of flow
489 cessation), consistent with another study showing elevated p27 levels after 16 hr of flow
490 [48], and percent p27+ cells then decreased during the remaining time and were almost
491 undetectable at 72 hr **(Fig. 4c-d, Supp. Fig. 5a).** Levels of p21, another member of the
492 CIP-KIP cell cycle inhibitor family, showed a similar decrease in levels even earlier in
493 the time course **(Fig. 4c, e, Supp. Fig. 5b**), and Ki67+ cells also decreased to
494 undetectable levels over flow time **(Fig. 4c,f; Supp. Fig 5c)**, consistent with the
495 conclusion that endothelial cells leave the cell cycle and become quiescent by 16-24hr
496 of laminar flow, then subsequently down-regulate p27 levels while maintaining
497 quiescence.
498
499 We then asked whether the quiescence depth of endothelial cells under laminar
500 flow was temporally regulated, by assessing time to cell cycle re-entry upon flow
501 cessation after 16 hr of flow (flow establishment (Flow-E)), a timepoint showing elevated
502 levels of p27. After this relatively short exposure to laminar flow, endothelial cells did not

503 exhibit significant EdU-labeling and pRB reactivity until 8 hr post-flow, similar to
504 endothelial cells released from contact inhibition and longer than the 2 hr time to cell
505 cycle re-entry exhibited by endothelial cells exposed to extended laminar flow (Flow-M)
506 **(Fig. 4g-i; Supp. Fig. 5d)**. These findings correlate with the temporal regulation of p27
507 levels over the flow period, and they suggest that endothelial cells initially respond to
508 laminar flow by p27 upregulation and establishment of a relatively "deep" quiescence
509 (Flow-E) that over time becomes shallower, along with reduced levels of cell cycle
510 inhibitors p27 and p21. We further characterized the flow response by assessment of
511 endothelial cell alignment, which was not established at 16 hr of flow (Flow-E) but was
512 established by 72 hr of flow (Flow-M) in our model (**Supp. Fig. 5e-f).** Thus, endothelial
513 cells under laminar flow transition from a deep to a shallower quiescence over time,
514 coincident with flow-mediated cell alignment and reduced levels of p27.
515

516 **Transcriptional targets of flow-mediated endothelial cell signaling regulate p27**
517 **levels under laminar flow**

518
519 To better understand how endothelial cell p27 expression decreases over time
520 with laminar flow, we examined genes whose expression is upregulated by laminar flow
521 and whose encoded proteins transcriptionally repress p27. It is well-established that
522 signaling pathways such as Notch and BMP are upregulated with laminar flow [2,9,10], and
523 this in turn leads to upregulation of targets of these pathways. *ID3* and *HES1* are
524 downstream targets of the Notch and BMP pathways, respectively, and both
525 transcriptionally repress *CDKN1B* expression via direct promoter interactions [49,50]. Upon
526 exposure to extended laminar flow (Flow-M), we observed an accumulation of *HES1*

527 and *ID3* RNA via RT-qPCR compared to static conditions (**Supp. Fig. 6a-b**). We directly
528 assessed the effects of these transcription factors on p27 levels in endothelial cells via
529 siRNA KD and found that depletion of either *HES1* or *ID3* RNA prevented the normal
530 decrease in the percent of p27+ cells under extended laminar flow (Flow-M) **(Fig. 5a-b;**
531 **Supp. Fig. 6c)**, indicating that these repressors are required for flow-mediated
532 reduction of p27 levels over time.
533
534 We hypothesized that *HES1* and *ID3* are required for the temporal changes to
535 endothelial cell quiescence depth over time, and we predicted that *HES1* or *ID3*
536 depletion would prevent the transition from deep to shallower quiescence depth with
537 time. We performed cell cycle re-entry experiments upon cessation of extended laminar
538 flow (Flow-M) and found that either *HES1* or *ID3* depletion significantly extended the
539 time required to see significant increase in percent EdU+ and pRB+ endothelial cells
540 compared to controls (**Fig. 5c-h, Supp. Fig. 6d-e),** suggesting that the normal change
541 to a shallow quiescence depth over time was prevented when these repressors were
542 depleted. These findings are consistent with the idea that endothelial quiescence depth
543 is temporally regulated from deep to shallow over time in conjunction with laminar flow-
544 mediated changes, and that p27 regulates this transition downstream of the
545 transcriptional repressors *HES1* and *ID3*.
546
547
548 **Endothelial cell p27 expression decreases with age *in vivo***
549
550 To begin to determine whether the transition from deep to shallow quiescence
551 documented here was mirrored *in vivo*, we used endothelial cell p27 expression as a

552 surrogate for quiescence depth and re-analyzed a published scRNAseq dataset
553 collected from mice of different ages[35]. We predicted higher levels *of Cdkn1b* in
554 endothelial cells of young mice with expanding vessel networks that are not yet
555 established, and we found that *Cdkn1b* expression was significantly higher in
556 endothelial cells from 1-month old mice compared to endothelial cells of older mice (3 or
557 18 months) **(Fig. 6a)**. Next, we analyzed temporal scRNAseq data we generated and
558 found that percent *Cdkn1b*+ endothelial cells in ear skin trended lower (p=0.16) with age
559 from neonatal (postnatal day 8) to adult (2-2.5 months) mice **(Fig. 6b)**. These findings
560 are consistent with the idea that endothelial cell quiescence depth changes with
561 developmental time, and that establishment initiates a deep quiescence that becomes
562 shallower over time as endothelial cells are exposed to extended laminar flow that
563 upregulates repressors of p27 expression (**Fig. 6c**).
564
565

566 **DISCUSSION**

567 Endothelial cell quiescence is important for vascular homeostasis and proper
568 barrier function, but how this quiescence is set up and maintained is not well-
569 understood. Here we show that quiescence depth is shallow in endothelial cells
570 exposed to extended laminar flow under maintenance conditions compared to contact-
571 inhibited endothelial cell quiescence depth in the absence of flow, and that flow-
572 mediated quiescence depth moves from a deeper to a shallower state as the
573 establishment phase ends and the maintenance phase commences. This discovery is
574 unexpected because we originally presumed that cells exit the cell cycle to a shallow
575 quiescent state that becomes deeper over time rather than the opposite. This surprising
576 finding correlates with changes in expression of the cell cycle inhibitor p27 and requires
577 transcriptional repressors normally upregulated by laminar flow, and it suggests a new
578 critical control point for vascular homeostasis that is linked to aging [51–53].
579

580 To better understand how endothelial cell quiescence varies with stimulus and
581 conditions, we developed an endothelial quiescence score using a cohort of genes
582 primarily chosen because the encoded proteins are flow-regulated and involved in the
583 cell cycle [8]. Application of this score to bulk RNA seq data not used to generate the
584 score validated that it was higher in endothelial cells predicted to be quiescent.
585 Moreover, application of a unique quiescence score developed by the Barr lab for
586 epithelial cells found similar relationships [54], suggesting that some aspects of vascular
587 quiescence are shared among cell types and conditions. Both quiescence scores were
588 higher in endothelial cells made quiescent via extended laminar flow or contact

589 inhibition compared to controls, and further transcriptome analysis revealed that both
590 conditions were characterized by down-regulation of cell cycle activators while only
591 contact inhibited endothelial cells showed increased expression of cell cycle inhibitor
592 genes. Further analysis of bulk RNAseq data indicated that although exposure to
593 extended flow or contact inhibition led to about a quarter of differentially regulated
594 genes being shared, most were unique to the quiescence stimulus, and comparison of
595 the most highly regulated genes and GO categories supported that the transcriptional
596 profiles are largely unique to flow or contact inhibition.
597
598 The global differences in cell cycle inhibitor expression in extended flow- vs.
599 contact inhibition-mediated quiescence correlated with expression of the cell cycle
600 inhibitor p27, and quiescence depth experiments revealed that endothelial cells under
601 extended laminar flow reentered the cell cycle soon after flow cessation while released
602 contact inhibited cells took significantly longer, indicating a deeper quiescence state.
603 This was surprising, as intuitively vascular homeostasis associated with extended
604 laminar flow was thought to be accompanied by relatively deep quiescence, and
605 endothelial cells exposed to laminar flow are in a high density monolayer. However,
606 these findings positively correlated with p27 levels, and reanalysis of several RNA seq
607 datasets showed a trend of reduced endothelial cell p27 levels with age. This is in line
608 with a recent study that found high levels of interstitial flow associated with shallower
609 quiescence in fibroblasts [55]. In another study, quiescence depth was invoked to explain
610 *in vivo* findings, as muscle stem cells entered a shallow quiescence state in response to

611 injury, and the shallow quiescence was proposed to be advantageous in wound
612 resolution [24].
613
614 Reduced p27 expression in endothelial cells exposed to extended flow was
615 nevertheless accompanied by a functional requirement for p27 to establish quiescence,
616 suggesting different requirements for the establishment vs. maintenance of vascular
617 quiescence. Direct analysis showed that quiescence depth changed with exposure time
618 to laminar flow, starting with a deep quiescence during the establishment phase (Flow-
619 E) when endothelial cells were not yet aligned to the flow vector, and becoming shallow
620 over extended exposure (Flow-M) and cell alignment to flow, consistent with our model
621 invoking distinct requirements for establishment vs. maintenance of laminar flow-
622 mediated endothelial quiescence. This idea is also consistent with our finding that p27
623 levels vary temporally during flow-mediated quiescence, increasing over the first 16-24
624 hours of laminar flow exposure and decreasing to very low levels with further flow.
625 Taken together, these data suggest that flow-mediated quiescence exhibits different
626 requirements for establishment vs. maintenance, and that the functional requirement for
627 p27 is related to establishment but not maintenance of flow-mediated quiescence. This
628 phenomenon is unique to flow, as both we and others have found that under high
629 density contact-inhibited endothelial cells accumulate p27 [43].
630
631 p27 expression is regulated by transcriptional repressors that are in turn
632 positively regulated by laminar flow, suggesting how endothelial cell p27 levels are
633 dynamically regulated in response to laminar flow **(Fig 6c)**. Both Notch and BMP

634 signaling are flow-regulated [9,10], and *HES1* and *ID3* are known transcriptional targets of
635 Notch and BMP, respectively, that are upregulated with laminar flow [56–58]. We found that
636 both repressors are functionally required non-redundantly to dampen p27 expression as
637 endothelial cells move from the establishment phase to the maintenance phase of
638 quiescence and vascular homeostasis. Endothelial cell quiescence depth is more
639 profound in the absence of either repressor, indicating that increased Notch and BMP
640 signaling during quiescence establishment, and subsequent upregulation of these
641 repressors leads to reduced p27 expression levels and a change from a deep to shallow
642 endothelial quiescence depth. This model is consistent with a defined role for p27-
643 mediated cell cycle regulation during angiogenesis to promote arterio-venous
644 differentiation important for early stages of angiogenesis and remodeling [48,59]. It is also
645 consistent with our analysis of RNA seq data showing decreased endothelial cell p27
646 levels with age, since age is predicted to result in more endothelial cells in the
647 maintenance phase of vascular quiescence.
648
649 Our work shows that endothelial cells have different responses to quiescence-
650 inducing stimuli. Quiescence depth changes over time from deep to shallow with
651 laminar flow, and this temporal regulation requires upregulation of p27 repressors and
652 reduced levels of p27 protein. Why might there be an advantage to endothelial cells
653 supporting a shallower quiescence state under flow maintenance (homeostasis)
654 conditions? One possibility is protection from premature senescence. Senescent cells
655 are permanently arrested [60], and fibroblasts that remain in quiescence for extended
656 periods of time eventually undergo senescence [61]. Senescent endothelial cells often

657 express a senescence-associated secretory phenotype (SASP) [62] that includes
658 upregulation of inflammatory cytokines that contribute to endothelial dysfunction,
659 leading to cardiovascular disease [63–65]. Thus, endothelial cells in a shallow quiescence
660 state at steady state may be protected from inappropriate senescence. *HES1*
661 expression in fibroblasts prevents premature senescence [66], supporting the concept that
662 shallow quiescence may protect from senescence.
663
664 A shallower endothelial cell quiescence depth may also help promote
665 physiological angiogenesis. A seminal study showed that endothelial cells *in vivo* are
666 non-proliferative but can respond to angiogenic/growth signals and re-enter the cell
667 cycle relatively quickly [67]. It was posited that these properties set up vascular
668 homeostasis while allowing for endothelial cells to rapidly respond to physiological or
669 pathological signals for angiogenesis. More recent work provides evidence that some
670 endothelial cells in the dorsal aorta respond to clamp injury with clonal expansion to
671 cover the denuded area in a relatively short time period [68]. Thus, the need to
672 simultaneously maintain homeostasis yet be primed for prompt injury response may be
673 facilitated by a relatively shallow endothelial cell quiescence depth. Conversely, shallow
674 quiescence depth may also contribute to pathological neo-angiogenesis associated with
675 diseases such as cancer.
676
677

ACKNOWLEDGMENTS

We thank members of the Bautch and Cook labs for their support and feedback, and the UNC High Throughput Sequencing Core for technical help with bulk RNAseq sample preparation and sequencing. We thank BioRender for figure model generation.

AUTHOR CONTRIBUTIONS

Natalie T Tanke (NTT), Jeanette Gowen Cook (JGC), Victoria L Bautch (VLB) conceptualized the work; NTT, Ziqing Liu (ZL), Morgan Oatley (MO), Tianji Yu (TY), Pauline Bougaran (PB), and Kaitlyn Quigley (KQ) performed and analyzed experiments. NTT and VLB wrote and edited the manuscript; VLB and JGC provided study supervision and oversight.

FUNDING

This work was supported by grants from the National Institutes of Health (R35 HL139950 to VLB), the MiBioX T32 Training Grant (T32 GM 119999-03, NTT), a Ruth L. Kirschstein Predoctoral Fellowship (1F31HL156527-01 to NTT), and an American Heart Association Postdoctoral Fellowship (AHA829371 to MO).

DECLARATION OF INTERESTS: none

699 **FIGURE LEGENDS**
700
701 **Figure 1. Laminar flow-mediated quiescence is transcriptionally distinct.**

702 **(a)** Quantification of epithelial quiescence score in HUVEC scRNA dataset by cluster.
703 Clusters were previously defined[8]. Flow-M, flow maintenance (laminar flow
704 (15d/cm^2/72hr)). Static cells were visually checked for subconfluence and fixed 48 hr
705 post-seeding. **(b)** Quantification of endothelial quiescence score in HUVEC scRNA
706 dataset by cluster. **(c)** Endothelial quiescence score on bulk RNA seq data of HUVEC
707 exposed to indicated stimuli, n= 3 replicates. **(d-e)** Heatmaps showing relative
708 expression of cell cycle proliferation markers (green font) and inhibitors (red font) plotted
709 using bulk RNAseq data of HUVEC under indicated conditions, n=3 replicates.
710 Statistics, one-way ANOVA with Tukey's multiple comparison test; ** $p \leq 0.01$, *** $p \leq$
711 0.001, ****$p \leq 0.0001$, *ns = not significant*.
712
713
714 **Figure 2. Endothelial cell flow maintenance quiescence stimulus leads to shallow**
715 **quiescence depth.**

716 **(a)** Representative images of HUVEC under static (non-flow) or Flow-M (flow
717 maintenance) conditions with EdU incorporation and fixation at indicated times post
718 Flow-M release. Cultures stained for DAPI (white, nuclear mask) and EdU (red, s-
719 phase) or pRB (blue, interphase). Scale bar, 50 μm. White arrow, flow direction. **(b)**
720 Quantification of percent EdU+ cells with indicated conditions. n=3 replicates, 5 images
721 per condition per replicate. **(c)** Quantification of percent pRB+ cells with indicated
722 conditions. n=3 replicates, 5 images per condition per replicate. **(d)** Representative
723 images of HUVEC under low or high density conditions with EdU incorporation and

724 fixation at indicated times post high-density release. Cultures stained for DAPI (white,
725 nuclear mask) and EdU (red, s-phase) or pRB (blue, interphase). Scale bar, 50 μm. **(e)**
726 Quantification of percent EdU+ cells with indicated conditions. n=3 replicates, 6 images
727 per condition per replicate. **(f)** Quantification of percent pRB+ cells with indicated
728 conditions. n=3 replicates, 6 images per condition per replicate. Statistics, one-way
729 ANOVA with Tukey's multiple comparisons test; *$p \leq 0.05$, ** $p \leq 0.01$, *** $p \leq 0.001$,
730 ****$p \leq 0.0001$, ns = not significant*.

731
732
733 **Figure 3. Cell cycle inhibitor p27 expression levels vary with endothelial**
734 **quiescence stimulus.**
735 **(a)** RT-qPCR for *CDKN1B* levels in indicated conditions. n=3 replicates. **(b)**
736 Representative images of HUVEC under indicated conditions stained for p27 (green)
737 and DAPI (white, nuclear mask). Scale bar, 50 μm. White arrow, flow direction. **(c)**
738 Quantification of HUVEC p27+ cells under indicated conditions, n=3 replicates, 5
739 images per condition per replicate. **(d)** RT-qPCR for *CDKN1B* levels in indicated
740 conditions. n=3 replicates. **(e)** Representative images of HUVEC under indicated
741 conditions stained for p27 (green) and DAPI (white, nuclear mask). Scale bar, 50 μm. **(f)**
742 Quantification of HUVEC p27+ cells under indicated conditions. n=3 replicates, 5
743 images per condition per replicate. Statistics, student's two-tailed *t*-test; ** $p \leq 0.01$,
744 ****$p \leq 0.0001$.

745

746

747 **Figure 4. Endothelial quiescence depth varies with laminar flow exposure time**
748 **and positively correlates with p27 expression levels**
749
750 **(a)** Representative images of HUVEC with indicated siRNA treatments and conditions.
751 after EdU incorporation (red, S-phase) and staining with DAPI (white, nuclear mask).
752 Scale bar, 50 μm. White arrow, flow direction. **(b)** Quantification of EdU+ cells with
753 indicated conditions. n=3 replicates, 5 images per condition per replicate. **(c)**
754 Representative images of HUVEC with indicated conditions and stained for p27
755 (inhibitor), p21 (inhibitor), Ki67 (proliferation marker), and DAPI (nucleus) in white. Scale
756 bar, 50 μm. White arrow, flow direction. **(d-f)** Quantification of percent p27+ (d), p21+
757 cells (e), or Ki67+ cells (f). n=3 replicates, 5 images per condition per replicate, **(g)**
758 Representative images of HUVEC under indicted conditions and after EdU incorporation
759 (red, S-phase) and stained for pRB (blue, interphase) and with DAPI (white, nuclear
760 mask), Flow-E, flow establishment; Flow-M, flow maintenance. Scale bar, 50 μm. White
761 arrow, flow direction. **(h)** Quantification of EdU+ cells in indicated conditions. n=3
762 replicates, 5 images per condition per replicate. **(i)** Quantification of pRB+ cells in
763 indicated conditions. n=3 replicates, 5 images per condition per replicate. Statistics,
764 one-way ANOVA with Tukey's multiple comparisons test; *$p \leq 0.05$, ****$p \leq 0.0001$, *ns* =
765 *not significant*.
766
767 **Figure 5. BMP and NOTCH regulated p27 repressors *HES1* and *ID3* regulate p27**
768 **levels and flow-mediated quiescence depth**
769 **(a)** Representative images of HUVEC under indicated conditions and with indicated
770 siRNA treatment. Cells stained for p27 (green) and DAPI (white, nuclear mask). Scale

771 bar, 50 μm. White arrow, flow direction. **(b)** Quantification of p27+ cells under indicated
772 conditions and treatments. n=3 replicates, 5 images per condition per replicate. **(c)**
773 Representative images of HUVEC with indicated conditions and siRNA treatments.
774 Cells were pulse labeled with EdU (red, S-phase) and stained for pRB (blue, interphase)
775 and DAPI (white, nuclear mask). Scale bar, 50 μm. White arrow, flow direction. **(d)**
776 Representative images of HUVEC with indicated conditions and siRNA treatments.
777 Cells were pulse labeled with EdU (red, S-phase) and stained for pRB (blue, interphase)
778 and DAPI (white, nuclear mask). Scale bar, 50 μm. White arrow, flow direction. **(e)**
779 Quantification of EdU+ cells with indicated conditions. n=3 replicates, 5 images per
780 condition per replicate. **(f)** Quantification of pRB+ cells with indicated conditions. n=3
781 replicates, 5 images per condition per replicate. **(g)** Quantification of EdU+ cells with
782 indicated conditions. n=3 replicates, 5 images per condition per replicate. **(h)**
783 Quantification of pRB+ positive cells with indicated conditions. n=3 replicates, 5 images
784 per condition per replicate. Statistics, one-way ANOVA with Tukey's multiple
785 comparisons test. ** $p \leq 0.01$, *** $p \leq 0.001$, ****$p \leq 0.0001$, *ns = not significant*.
786
787

788 **Figure 6. *Cdkn1b* expression does not accumulate with age *in vivo***
789 **(a)** scRNAseq analysis of normalized *Cdkn1b* expression in endothelial cells isolated
790 from mice of indicated ages. See Methods and text for details of dataset reanalysis.
791 Endothelial cells with *Cdkn1b* expression at 0 were excluded from analysis. ****$p \leq$
792 *0.0001, ns = not significant* by one-way ANOVA with Tukey's multiple comparisons test.
793 **(b)** scRNAseq analysis of percent *Cdkn1b*+ endothelial cells isolated from neonatal (P8)
794 or adult (2-2.5m) murine ears. Each dot represents one endothelial subpopulation in

795 one sample. Statistics, student's two-tailed *t*-test **(c)** Proposed model for dynamic
796 regulation of endothelial cell flow-mediated quiescence depth with flow exposure time.
797 In the first 16-24 hr (Flow-E, flow establishment), a deep quiescence is established
798 accompanied by high levels of cell cycle inhibitor p27. With time, transcription factors
799 that are targets of flow-mediated Notch and BMP signaling are upregulated, and these
800 p27 transcriptional repressors prevent ongoing p27 synthesis and lead to significantly
801 reduced p27 levels. The regulators are required to transition to a shallow quiescence
802 depth that characterizes extended exposure to laminar flow (Flow-M, flow
803 maintenance).
804
805

806 **SUPPLEMENTARY FIGURE LEGENDS**
807
808 **Supplemental Figure 1. Endothelial bulk RNAseq-derived quiescence**
809 **transcriptional profiles are distinct with different stimuli.**
810 **(a)** Quantification of an epithelial quiescence score [54] of HUVEC bulk RNAseq dataset
811 from different conditions. Statistics, *$p \leq 0.05$ using One-Way ANOVA with Tukey's
812 multiple comparison test, n=3 replicates. Flow-M, flow maintenance. **(b)** Venn diagrams
813 showing bulk RNA seq analysis of genes up- and down-regulated in HUVEC under
814 indicated conditions. **(c-f)** Heatmaps showing relative expression levels of genes (top 50
815 by fold change and p-value) in bulk RNA seq from HUVEC under indicated conditions.
816 **(g-j)** GO term analysis from bulk RNA-seq data with indicated comparisons.
817 Representative biological processes GO terms significantly enriched (P adjusted < 0.1)
818 in differentially regulated genes are shown.
819
820 **Supplemental Figure 2. pRB nuclear fluorescence intensity under indicated**
821 **conditions.**
822 **(a)** Schematic showing areas of scratch wound used for imaging post-scratch for
823 contact inhibition quiescence depth experiments. **(b)** Quantification of pRB nuclear
824 fluorescence intensity under indicated conditions. n=3 replicates, 5 images averaged
825 per condition per replicate. **(c)** Quantification of nuclear fluorescence intensity of pRB in
826 low vs. high density release timepoints. n=3 replicates, n=5 averaged images per
827 condition per replicate. Statistics, one-way ANOVA with Tukey's multiple comparisons
828 test *$p \leq 0.05$, ** $p \leq 0.01$, *** $p \leq 0.001$, ****$p \leq 0.0001$, *ns= not significant*.
829

830 **Supplemental Figure 3. Cell cycle inhibitor p27 expression differs with**
831 **quiescence stimulus.**
832
833 **(a)** Quantification of p27 nuclear fluorescence intensity in indicated conditions. n=3
834 replicates, 5 images averaged per condition per replicate. **(b)** Quantification of p27
835 nuclear fluorescence intensity in indicated conditions. n=3 replicates, 5 images
836 averaged per condition per replicate. **(c)** Western blot of p27 expression under indicated
837 conditions, and with indicated antibodies. p27 Ab #1 (Cell Signaling) and p27 Ab #2
838 (Santa Cruz). **(d)** Representative images of HUVEC with indicated siRNA and
839 treatments. Endothelial cells stained with Ki67 (yellow, proliferation marker) and DAPI
840 (gray, nucleus mask). Scale bar 50 μm. White arrow, flow direction. **(e)** Quantification of
841 percent Ki67+ cells. n=3 replicates, n= 5 images per condition per replicate. **(f)**
842 Quantification of nuclear fluorescence intensity of Ki67. n=3 replicates, n=5 averaged
843 images per condition per replicate. Statistics, one-way ANOVA with Tukey's multiple
844 comparisons test; *** $p \leq 0.01$, ****$p \leq 0.0001$, ns= not significant*.
845
846 **Supplemental Figure 4. p27 depletion leads to distinct transcriptional changes**
847 **dependent on quiescence stimulus.**
848 **(a)** Venn diagrams showing overlap of HUVEC genes differentially regulated in
849 indicated conditions and for *CDKN1B* KD compared to NT. **(b-e)** Heatmaps showing
850 relative expression levels of genes differentially regulated (top 50 by fold change and p-
851 value) in response to indicated conditions. **(f-i)** GO analysis performed on differentially
852 expressed genes from bulk RNA-seq data under comparing indicated

853 conditions/treatments. Representative biological processes GO terms significantly
854 enriched (P adjusted < 0.1) in differentially regulated genes are shown.
855
856
857 **Supplemental Figure 5. Cell cycle inhibitor and Ki67 expression intensity varies**
858 **with flow exposure and correlates with flow-mediated endothelial cell alignment**.
859 **(a)** Quantification of p27 nuclear fluorescence intensity with indicated conditions. n=3
860 replicates, 5 averaged images per condition per replicate. **(b)** Quantification of p21
861 nuclear fluorescence intensity with indicated conditions. n=3 replicates, 5 averaged
862 images per condition per replicate. **(c)** Quantification of Ki67 nuclear fluorescence
863 intensity with indicated conditions. n=3 replicates, 5 averaged images per condition per
864 replicate. **(d)** Quantification of pRB nuclear fluorescence intensity under indicated
865 conditions. n=3 replicates, 5 averaged images per condition per replicate. **(e)**
866 Representative images of HUVEC stained with VE-cadherin (white, junction marker)
867 and DAPI (blue, nucleus) under indicated conditions. Scale bar, 50 μm. White arrow,
868 flow direction. **(f)** Cell axis ratio quantification in indicated conditions. n=3 replicates, 5
869 images per condition per replicate. Statistics, one-way ANOVA with Tukey's multiple
870 comparisons test; *$*p \leq 0.05$, $**p \leq 0.01$, $***\ p \leq 0.001$, $****p \leq 0.0001$, ns = not*
871 *significant*.
872
873 **Supplemental Figure 6. Nuclear fluorescence intensity of markers and changes**
874 **with *HES1* or *ID3* depletion.**
875 **(a)** RT-qPCR for *HES1* expression under indicated conditions. n=3 replicates. Statistics,
876 $***\ p \leq 0.001$ with student's two-tailed *t*-test. **(b)** RT-qPCR for *ID3* expression under

877 indicated conditions, n=3 replicates. Statistics, * $p \leq 0.05$ with student's two-tailed *t*-test.
878 **(c)** Quantification of p27 nuclear fluorescence intensity with indicated siRNA treatments
879 and conditions. n=3 replicates, 5 averaged images per condition per replicate. Statistics,
880 ** $p \leq 0.01$, **** $p \leq 0.0001$ by one-way ANOVA with Tukey's multiple comparisons test.
881 **(d)** Quantification of pRB nuclear fluorescence intensity with indicated siRNA treatments
882 and conditions. n=3 replicates, 5 averaged images per condition per replicate. Statistics,
883 **** $p \leq 0.0001$, *ns= not significant* by one-way ANOVA with Tukey's multiple comparisons
884 test. **(e)** Quantification of pRB nuclear fluorescence intensity with indicated siRNA
885 treatments and conditions. n=3 replicates, 5 averaged images per condition per
886 replicate. Statistics, ** $p \leq 0.01$, **** $p \leq 0.0001$, *ns= not significant* by one-way ANOVA
887 with Tukey's multiple comparisons test.
888

889 **REFERENCES**
890

891 1. Privratsky JR, Newman PJ. PECAM-1: regulator of endothelial junctional integrity.
892 *Cell Tissue Res*. 2014;355(3):607-619. doi:10.1007/s00441-013-1779-3

893 2. Baeyens N, Schwartz MA. Biomechanics of vascular mechanosensation and
894 remodeling. *Mol Biol Cell*. 2016;27(1):7-11. doi:10.1091/mbc.E14-11-1522

895 3. Sluysmans S, Vasileva E, Spadaro D, Shah J, Rouaud F, Citi S. The role of apical
896 cell-cell junctions and associated cytoskeleton in mechanotransduction. *Biol Cell*.
897 2017;109(4):139-161. doi:10.1111/boc.201600075

898 4. Levesque MJ, Sprague EA, Schwartz CJ, Nerem RM. The Influence of Shear
899 Stress on Cultured Vascular Endothelial Cells: The Stress Response of an
900 Anchorage-Dependent Mammalian Cell. *Biotechnol Prog*. 1989;5(1):1-8.
901 doi:10.1002/btpr.5420050105

902 5. Levesque MJ, Nerem RM, Sprague EA. Vascular endothelial cell proliferation in
903 culture and the influence of flow. *Biomaterials*. 1990;11(9):702-707.
904 doi:10.1016/0142-9612(90)90031-k

905 6. Ziegler T, Nerem RM. Effect of flow on the process of endothelial cell division.
906 *Arterioscler Thromb J Vasc Biol*. 1994;14(4):636-643. doi:10.1161/01.atv.14.4.636

907 7. Ruter DL, Liu Z, Ngo KM, X S, Marvin A, Buglak DB, Kidder EJ, Bautch VL.
908 SMAD6 transduces endothelial cell flow responses required for blood vessel
909 homeostasis. *Angiogenesis*. 2021;24(2):387-398. doi:10.1007/s10456-021-09777-7

910 8. Liu Z, Ruter DL, Quigley K, Tanke NT, Jiang Y, Bautch VL. Single-Cell RNA
911 Sequencing Reveals Endothelial Cell Transcriptome Heterogeneity Under
912 Homeostatic Laminar Flow. *Arterioscler Thromb Vasc Biol*. 2021;41(10):2575-
913 2584. doi:10.1161/ATVBAHA.121.316797

914 9. Yang J, Li X, Li Y, Southwood M, Ye L, Long L, Al-Lamki RS, Morrell NW. Id
915 proteins are critical downstream effectors of BMP signaling in human pulmonary
916 arterial smooth muscle cells. *Am J Physiol - Lung Cell Mol Physiol*.
917 2013;305(4):L312-L321. doi:10.1152/ajplung.00054.2013

918 10. Jouve C, Palmeirim I, Henrique D, Beckers J, Gossler A, Ish-Horowicz D, Pourquie
919 O. Notch signalling is required for cyclic expression of the hairy-like gene HES1 in
920 the presomitic mesoderm. *Development*. 2000;127(7):1421-1429.
921 doi:10.1242/dev.127.7.1421

922 11. Caplan BA, Schwartz CJ. Increased endothelial cell turnover in areas of in vivo
923 Evans Blue uptake in the pig aorta. *Atherosclerosis*. 1973;17(3):401-417.
924 doi:10.1016/0021-9150(73)90031-2

925 12. Schlereth K, Weichenhan D, Bauer T, Heumann T, Giannakouri E, Lipka D, Jaeger
926 S, Schlesner M, Aloy P, Eils R, Plass C, Augustin HG. The transcriptomic and
927 epigenetic map of vascular quiescence in the continuous lung endothelium. *eLife*.
928 2018;7:e34423. doi:10.7554/eLife.34423

929 13. Millauer B, Wizigmann-Voos S, Schnürch H, Martinez R, Møller NPH, Risau W,
930 Ullrich A. High affinity VEGF binding and developmental expression suggest Flk-1
931 as a major regulator of vasculogenesis and angiogenesis. *Cell*. 1993;72(6):835-
932 846. doi:10.1016/0092-8674(93)90573-9

933 14. Gerhardt H, Golding M, Fruttiger M, Ruhrberg C, Lundkvist A, Abramsson A,
934 Jeltsch M, Mitchell C, Alitalo K, Shima D, Betsholtz C. VEGF guides angiogenic
935 sprouting utilizing endothelial tip cell filopodia. *J Cell Biol*. 2003;161(6):1163-1177.
936 doi:10.1083/jcb.200302047

937 15. Bernatchez PN, Soker S, Sirois MG. Vascular Endothelial Growth Factor Effect on
938 Endothelial Cell Proliferation, Migration, and Platelet-activating Factor Synthesis Is
939 Flk-1-dependent *. *J Biol Chem*. 1999;274(43):31047-31054.
940 doi:10.1074/jbc.274.43.31047

941 16. Coller HA, Sang L, Roberts JM. A New Description of Cellular Quiescence. *PLOS*
942 *Biol*. 2006;4(3):e83. doi:10.1371/journal.pbio.0040083

943 17. Min M, Spencer SL. Spontaneously slow-cycling subpopulations of human cells
944 originate from activation of stress-response pathways. *PLoS Biol*.
945 2019;17(3):e3000178. doi:10.1371/journal.pbio.3000178

946 18. Johnson MS, Cook JG. Cell cycle exits and U-turns: Quiescence as multiple
947 reversible forms of arrest. *Fac Rev*. 2023;12:5. doi:10.12703/r/12-5

948 19. Hartwell LH, Culotti J, Pringle JR, Reid BJ. Genetic Control of the Cell Division
949 Cycle in Yeast. *Science*. 1974;183(4120):46-51. doi:10.1126/science.183.4120.46

950 20. Tarn WY, Lai MC. Translational control of cyclins. *Cell Div*. 2011;6:5.
951 doi:10.1186/1747-1028-6-5

952 21. MINSHULL J, PINES J, GOLSTEYN R, STANDART N, MACKIE S, COLMAN A,
953 BLOW J, RUDERMAN JV, WU M, HUNT T. The role of cyclin synthesis,
954 modification and destruction in the control of cell division. *J Cell Sci*.
955 1989;1989(Supplement_12):77-97. doi:10.1242/jcs.1989.Supplement_12.8

956 22. Kwon JS, Everetts NJ, Wang X, Wang W, Croce KD, Xing J, Yao G. Controlling
957 Depth of Cellular Quiescence by an Rb-E2F Network Switch. *Cell Rep*.
958 2017;20(13):3223-3235. doi:10.1016/j.celrep.2017.09.007

959 23. Fujimaki K, Li R, Chen H, Croce KD, Zhang HH, Xing J, Bai F, Yao G. Graded
960 regulation of cellular quiescence depth between proliferation and senescence by a

961 lysosomal dimmer switch. *Proc Natl Acad Sci*. Published online October 21, 2019.
962 doi:10.1073/pnas.1915905116

963 24. Rodgers JT, King KY, Brett JO, Cromie MJ, Charville GW, Maguire KK, Brunson C,
964 Mastey N, Liu L, Tsai CR, Goodell MA, Rando TA. mTORC1 controls the adaptive
965 transition of quiescent stem cells from G0 to GAlert. *Nature*. 2014;510(7505):393-
966 396. doi:10.1038/nature13255

967 25. Min M, Rong Y, Tian C, Spencer SL. Temporal integration of mitogen history in
968 mother cells controls proliferation of daughter cells. *Science*. 2020;368(6496):1261-
969 1265. doi:10.1126/science.aay8241

970 26. Schindelin J, Arganda-Carreras I, Frise E, Kaynig V, Longair M, Pietzsch T,
971 Preibisch S, Rueden C, Saalfeld S, Schmid B, Tinevez JY, White DJ, Hartenstein
972 V, Eliceiri K, Tomancak P, Cardona A. Fiji: an open-source platform for biological-
973 image analysis. *Nat Methods*. 2012;9(7):676-682. doi:10.1038/nmeth.2019

974 27. Dardik A, Chen L, Frattini J, Asada H, Aziz F, Kudo FA, Sumpio BE. Differential
975 effects of orbital and laminar shear stress on endothelial cells. *J Vasc Surg*.
976 2005;41(5):869-880. doi:10.1016/j.jvs.2005.01.020

977 28. Liang D, Chang JR, Chin AJ, Smith A, Kelly C, Weinberg ES, Ge R. The role of
978 vascular endothelial growth factor (VEGF) in vasculogenesis, angiogenesis, and
979 hematopoiesis in zebrafish development. *Mech Dev*. 2001;108(1):29-43.
980 doi:10.1016/S0925-4773(01)00468-3

981 29. Mahmood T, Yang PC. Western Blot: Technique, Theory, and Trouble Shooting.
982 *North Am J Med Sci*. 2012;4(9):429-434. doi:10.4103/1947-2714.100998

983 30. Buglak DB, Bougaran P, Kulikauskas MR, Liu Z, Monaghan-Benson E, Gold AL,
984 Marvin AP, Burciu A, Tanke NT, Oatley M, Ricketts SN, Kinghorn K, Johnson BN,
985 Shiau CE, Rogers S, Guilluy C, Bautch VL. Nuclear SUN1 stabilizes endothelial
986 cell junctions via microtubules to regulate blood vessel formation. Koh GY,
987 Akhmanova A, eds. *eLife*. 2023;12:e83652. doi:10.7554/eLife.83652

988 31. A D, Ca D, F S, J D, C Z, S J, P B, M C, Tr G. STAR: ultrafast universal RNA-seq
989 aligner. *Bioinforma Oxf Engl*. 2013;29(1). doi:10.1093/bioinformatics/bts635

990 32. Putri GH, Anders S, Pyl PT, Pimanda JE, Zanini F. Analysing high-throughput
991 sequencing data in Python with HTSeq 2.0. *Bioinforma Oxf Engl*.
992 2022;38(10):2943-2945. doi:10.1093/bioinformatics/btac166

993 33. Love MI, Huber W, Anders S. Moderated estimation of fold change and dispersion
994 for RNA-seq data with DESeq2. *Genome Biol*. 2014;15(12):550.
995 doi:10.1186/s13059-014-0550-8

996 34. Wiecek AJ, Cutty SJ, Kornai D, Parreno-Centeno M, Gourmet LE, Tagliazucchi
997 GM, Jacobson DH, Zhang P, Xiong L, Bond GL, Barr AR, Secrier M. Genomic

998 hallmarks and therapeutic implications of G0 cell cycle arrest in cancer. Published
999 online April 15, 2023:2021.11.12.468410. doi:10.1101/2021.11.12.468410

1000 35. Almanzar N, Antony J, Baghel AS, Bakerman I, Bansal I, Barres BA, Beachy PA,
1001 Berdnik D, Bilen B, Brownfield D, Cain C, Chan CKF, Chen MB, Clarke MF, Conley
1002 SD, Darmanis S, Demers A, Demir K, de Morree A, Divita T, du Bois H, Ebadi H,
1003 Espinoza FH, Fish M, Gan Q, George BM, Gillich A, Gòmez-Sjöberg R, Green F,
1004 Genetiano G, Gu X, Gulati GS, Hahn O, Haney MS, Hang Y, Harris L, He M,
1005 Hosseinzadeh S, Huang A, Huang KC, Iram T, Isobe T, Ives F, Jones RC, Kao KS,
1006 Karkanias J, Karnam G, Keller A, Kershner AM, Khoury N, Kim SK, Kiss BM, Kong
1007 W, Krasnow MA, Kumar ME, Kuo CS, Lam J, Lee DP, Lee SE, Lehallier B,
1008 Leventhal O, Li G, Li Q, Liu L, Lo A, Lu WJ, Lugo-Fagundo MF, Manjunath A, May
1009 AP, Maynard A, McGeever A, McKay M, McNerney MW, Merrill B, Metzger RJ,
1010 Mignardi M, Min D, Nabhan AN, Neff NF, Ng KM, Nguyen PK, Noh J, Nusse R,
1011 Pálovics R, Patkar R, Peng WC, Penland L, Pisco AO, Pollard K, Puccinelli R, Qi
1012 Z, Quake SR, Rando TA, Rulifson EJ, Schaum N, Segal JM, Sikandar SS, Sinha
1013 R, et al. A single-cell transcriptomic atlas characterizes ageing tissues in the
1014 mouse. *Nature*. 2020;583(7817):590-595. doi:10.1038/s41586-020-2496-1

1015 36. Chen BR, Cheng HH, Lin WC, Wang KH, Liou JY, Chen PF, Wu KK. Quiescent
1016 Fibroblasts Are More Active in Mounting Robust Inflammatory Responses Than
1017 Proliferative Fibroblasts. *PLOS ONE*. 2012;7(11):e49232.
1018 doi:10.1371/journal.pone.0049232

1019 37. Hayer A, Shao L, Chung M, Joubert LM, Yang HW, Tsai FC, Bisaria A, Betzig E,
1020 Meyer T. Engulfed cadherin fingers are polarized junctional structures between
1021 collectively migrating endothelial cells. *Nat Cell Biol*. 2016;18(12):1311-1323.
1022 doi:10.1038/ncb3438

1023 38. Lee HW, Xu Y, He L, Choi W, Gonzalez D, Jin SW, Simons M. Role of Venous
1024 Endothelial Cells in Developmental and Pathologic Angiogenesis. *Circulation*.
1025 2021;144(16):1308-1322. doi:10.1161/CIRCULATIONAHA.121.054071

1026 39. Lee HW, Shin JH, Simons M. Flow goes forward and cells step backward:
1027 endothelial migration. *Exp Mol Med*. 2022;54(6):711-719. doi:10.1038/s12276-022-
1028 00785-1

1029 40. Pereira PD, Serra-Caetano A, Cabrita M, Bekman E, Braga J, Rino J, Santus R,
1030 Filipe PL, Sousa AE, Ferreira JA. Quantification of cell cycle kinetics by EdU (5-
1031 ethynyl-2′-deoxyuridine)-coupled-fluorescence-intensity analysis. *Oncotarget*.
1032 2017;8(25):40514-40532. doi:10.18632/oncotarget.17121

1033 41. Goodrich DW, Wang NP, Qian YW, Lee EY, Lee WH. The retinoblastoma gene
1034 product regulates progression through the G1 phase of the cell cycle. *Cell*.
1035 1991;67(2):293-302. doi:10.1016/0092-8674(91)90181-w

1036 42. Buck SB, Bradford J, Gee KR, Agnew BJ, Clarke ST, Salic A. Detection of S-phase
1037 cell cycle progression using 5-ethynyl-2′-deoxyuridine incorporation with click

1038 chemistry, an alternative to using 5-bromo-2′-deoxyuridine antibodies.
1039 *BioTechniques*. 2008;44(7):927-929. doi:10.2144/000112812

1040 43. Noseda M, Chang L, McLean G, Grim JE, Clurman BE, Smith LL, Karsan A. Notch
1041 activation induces endothelial cell cycle arrest and participates in contact inhibition:
1042 role of p21Cip1 repression. *Mol Cell Biol*. 2004;24(20):8813-8822.
1043 doi:10.1128/MCB.24.20.8813-8822.2004

1044 44. Oesterle EC, Chien WM, Campbell S, Nellimarla P, Fero ML. p27(Kip1) is required
1045 to maintain proliferative quiescence in the adult cochlea and pituitary. *Cell Cycle*
1046 *Georget Tex*. 2011;10(8):1237-1248. doi:10.4161/cc.10.8.15301

1047 45. Besson A, Gurian-West M, Chen X, Kelly-Spratt KS, Kemp CJ, Roberts JM. A
1048 pathway in quiescent cells that controls p27Kip1 stability, subcellular localization,
1049 and tumor suppression. *Genes Dev*. 2006;20(1):47-64. doi:10.1101/gad.1384406

1050 46. Levenberg S, Yarden A, Kam Z, Geiger B. p27 is involved in N-cadherin-mediated
1051 contact inhibition of cell growth and S-phase entry. *Oncogene*. 1999;18(4):869-876.
1052 doi:10.1038/sj.onc.1202396

1053 47. Miller I, Min M, Yang C, Tian C, Gookin S, Carter D, Spencer SL. Ki67 is a Graded
1054 Rather than a Binary Marker of Proliferation versus Quiescence. *Cell Rep*.
1055 2018;24(5):1105-1112.e5. doi:10.1016/j.celrep.2018.06.110

1056 48. Fang JS, Coon BG, Gillis N, Chen Z, Qiu J, Chittenden TW, Burt JM, Schwartz MA,
1057 Hirschi KK. Shear-induced Notch-Cx37-p27 axis arrests endothelial cell cycle to
1058 enable arterial specification. *Nat Commun*. 2017;8. doi:10.1038/s41467-017-
1059 01742-7

1060 49. Chassot AA, Turchi L, Virolle T, Fitsialos G, Batoz M, Deckert M, Dulic V,
1061 Meneguzzi G, Buscà R, Ponzio G. Id3 is a novel regulator of p27kip1 mRNA in
1062 early G1 phase and is required for cell-cycle progression. *Oncogene*.
1063 2007;26(39):5772-5783. doi:10.1038/sj.onc.1210386

1064 50. Murata K, Hattori M, Hirai N, Shinozuka Y, Hirata H, Kageyama R, Sakai T, Minato
1065 N. Hes1 directly controls cell proliferation through the transcriptional repression of
1066 p27Kip1. *Mol Cell Biol*. 2005;25(10):4262-4271. doi:10.1128/MCB.25.10.4262-
1067 4271.2005

1068 51. Herrera MD, Mingorance C, Rodríguez-Rodríguez R, Alvarez de Sotomayor M.
1069 Endothelial dysfunction and aging: an update. *Ageing Res Rev*. 2010;9(2):142-152.
1070 doi:10.1016/j.arr.2009.07.002

1071 52. SEALS DR, JABLONSKI KL, DONATO AJ. Aging and vascular endothelial function
1072 in humans. *Clin Sci Lond Engl 1979*. 2011;120(9):357-375.
1073 doi:10.1042/CS20100476

1074 53. Donato AJ, Machin DR, Lesniewski LA. Mechanisms of Dysfunction in the Aging
1075 Vasculature and Role in Age-Related Disease. *Circ Res*. 2018;123(7):825-848.
1076 doi:10.1161/CIRCRESAHA.118.312563

1077 54. Wiecek AJ, Cutty SJ, Kornai D, Parreno-Centeno M, Gourmet LE, Tagliazucchi
1078 GM, Jacobson DH, Zhang P, Xiong L, Bond GL, Barr AR, Secrier M. Genomic
1079 hallmarks and therapeutic implications of cancer cell quiescence. *bioRxiv*.
1080 Published online January 1, 2022:2021.11.12.468410.
1081 doi:10.1101/2021.11.12.468410

1082 55. Liu B, Wang X, Jiang L, Xu J, Zohar Y, Yao G. Extracellular Fluid Flow Induces
1083 Shallow Quiescence Through Physical and Biochemical Cues. *Front Cell Dev Biol*.
1084 2022;10:792719. doi:10.3389/fcell.2022.792719

1085 56. Mack JJ, Mosqueiro TS, Archer BJ, Jones WM, Sunshine H, Faas GC, Briot A,
1086 Aragón RL, Su T, Romay MC, McDonald AI, Kuo CH, Lizama CO, Lane TF, Zovein
1087 AC, Fang Y, Tarling EJ, Vallim TQ de A, Navab M, Fogelman AM, Bouchard LS,
1088 Iruela-Arispe ML. NOTCH1 is a mechanosensor in adult arteries. *Nat Commun*.
1089 2017;8(1):1620. doi:10.1038/s41467-017-01741-8

1090 57. Helle E, Ampuja M, Antola L, Kivelä R. Flow-Induced Transcriptomic Remodeling of
1091 Endothelial Cells Derived From Human Induced Pluripotent Stem Cells. *Front*
1092 *Physiol*. 2020;11. Accessed April 7, 2023.
1093 https://www.frontiersin.org/articles/10.3389/fphys.2020.591450

1094 58. Zhang MJ, Pisco AO, Darmanis S, Zou J. Mouse aging cell atlas analysis reveals
1095 global and cell type-specific aging signatures. Han JDJ, Tyler JK, Hou L, eds. *eLife*.
1096 2021;10:e62293. doi:10.7554/eLife.62293

1097 59. Acharya BR, Fang JS, Jeffery ED, Chavkin NW, Genet G, Vasavada H, Nelson EA,
1098 Sheynkman GM, Humphries MJ, Hirschi KK. Connexin 37 sequestering of
1099 activated-ERK in the cytoplasm promotes p27-mediated endothelial cell cycle
1100 arrest. *Life Sci Alliance*. 2023;6(8). doi:10.26508/lsa.202201685

1101 60. Hayflick L, Moorhead PS. The serial cultivation of human diploid cell strains. *Exp*
1102 *Cell Res*. 1961;25(3):585-621. doi:10.1016/0014-4827(61)90192-6

1103 61. Marthandan S, Priebe S, Hemmerich P, Klement K, Diekmann S. Long-Term
1104 Quiescent Fibroblast Cells Transit into Senescence. *PLOS ONE*.
1105 2014;9(12):e115597. doi:10.1371/journal.pone.0115597

1106 62. Yin K, Patten D, Gough S, de Barros Gonçalves S, Chan A, Olan I, Cassidy L,
1107 Poblocka M, Zhu H, Lun A, Schuijs M, Young A, Martinez-Jimenez C, Halim TYF,
1108 Shetty S, Narita M, Hoare M. Senescence-induced endothelial phenotypes
1109 underpin immune-mediated senescence surveillance. *Genes Dev*. 2022;36(9-
1110 10):533-549. doi:10.1101/gad.349585.122

1111 63. Miyauchi H, Minamino T, Tateno K, Kunieda T, Toko H, Komuro I. Akt negatively
1112 regulates the in vitro lifespan of human endothelial cells via a p53/p21-dependent
1113 pathway. *EMBO J*. 2004;23(1):212-220. doi:10.1038/sj.emboj.7600045

1114 64. Chen Y, Liu Z, Chen H, Huang X, Huang X, Lei Y, Liang Q, Wei J, Zhang Q, Guo
1115 X, Huang Q. p53 SUMOylation Mediates AOPP-Induced Endothelial Senescence
1116 and Apoptosis Evasion. *Front Cardiovasc Med*. 2022;8. Accessed April 4, 2023.
1117 https://www.frontiersin.org/articles/10.3389/fcvm.2021.795747

1118 65. Minamino T, Miyauchi H, Yoshida T, Ishida Y, Yoshida H, Komuro I. Endothelial
1119 Cell Senescence in Human Atherosclerosis. *Circulation*. 2002;105(13):1541-1544.
1120 doi:10.1161/01.CIR.0000013836.85741.17

1121 66. Sang L, Coller HA, Roberts JM. Control of the reversibility of cellular quiescence by
1122 the transcriptional repressor HES1. *Science*. 2008;321(5892):1095-1100.
1123 doi:10.1126/science.1155998

1124 67. Ausprunk DH, Folkman J. Migration and proliferation of endothelial cells in
1125 preformed and newly formed blood vessels during tumor angiogenesis. *Microvasc*
1126 *Res*. 1977;14(1):53-65. doi:10.1016/0026-2862(77)90141-8

1127 68. McDonald AI, Shirali AS, Aragón R, Ma F, Hernandez G, Vaughn DA, Mack JJ, Lim
1128 TY, Sunshine H, Zhao P, Kalinichenko V, Hai T, Pelegrini M, Ardehali R, Iruela-
1129 Arispe ML. Endothelial Regeneration of Large Vessels Is a Biphasic Process
1130 Driven by Local Cells with Distinct Proliferative Capacities. *Cell Stem Cell*.
1131 2018;23(2):210-225.e6. doi:10.1016/j.stem.2018.07.011

1132
1133

1134 **Nonstandard Abbreviations and Acronyms**
1135
1136 HUVEC: Human Umbilical Vein Endothelial Cells
1137 Flow-M: Flow maintenance; 72 hr 15d/cm^2
1138 Flow-E: Flow establishment; 72 hr 15d/cm^2
1139 siRNA: Small interfering RNA
1140 KD: Knockdown
1141 A.U.: Arbitrary unit
1142 pRB: Phospho retinoblastoma protein
1143 EdU: 5-Ethynyl-2'-deoxyuridine
1144 *HES1*: Hes Family BHLH Transcription Factor 1
1145 *ID3*: Inhibitor of DNA Binding 3
1146

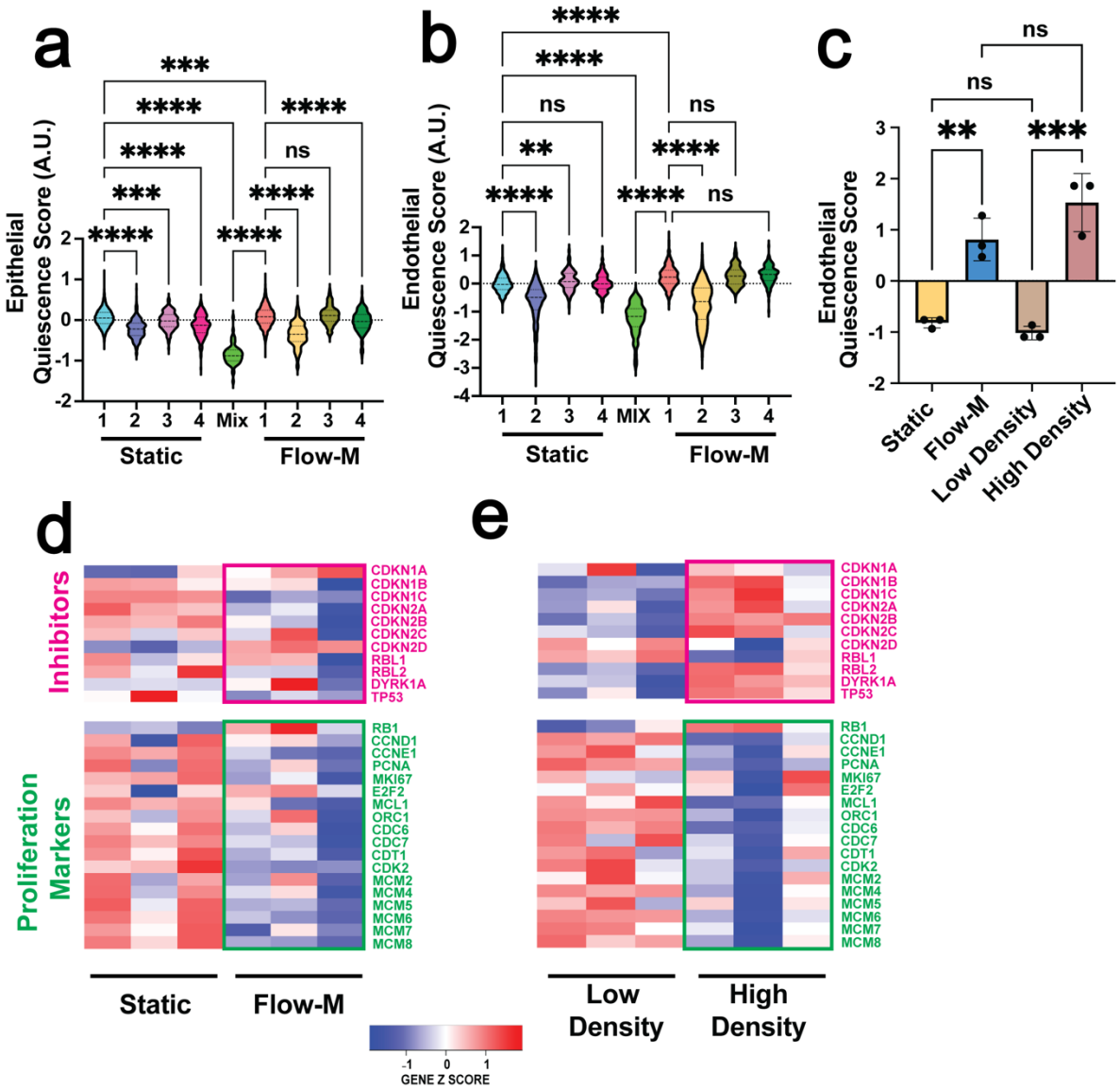

Figure 1. Laminar flow-mediated quiescence is transcriptionally distinct. **(a)** Quantification of epithelial quiescence score in HUVEC scRNA dataset by cluster. Clusters were previously defined[8]. Flow-M, flow maintenance (laminar flow (15d/cm^2/72hr)). Static cells were visually checked for subconfluence and fixed 48 hr post-seeding. **(b)** Quantification of endothelial quiescence score in HUVEC scRNA dataset by cluster. **(c)** Endothelial quiescence score on bulk RNA seq data of HUVEC exposed to indicated stimuli, n= 3 replicates. **(d-e)** Heatmaps showing relative expression of cell cycle proliferation markers (green font) and inhibitors (red font) plotted using bulk RNAseq data of HUVEC under indicated conditions, n=3 replicates. Statistics, one-way ANOVA with Tukey's multiple comparison test; ** $p \leq 0.01$, *** $p \leq 0.001$, ****$p \leq 0.0001$, *ns = not significant*.

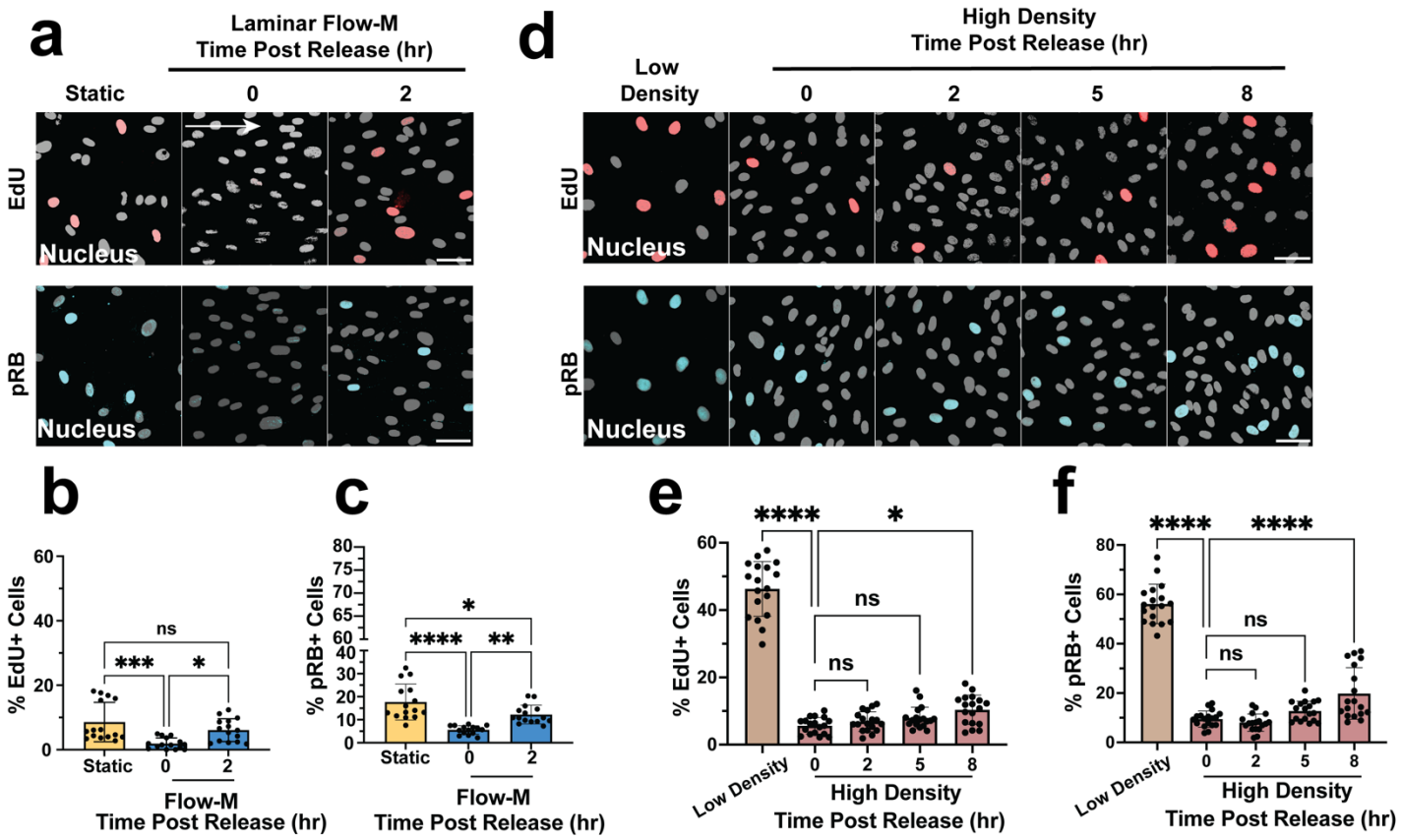

Figure 2. Endothelial cell flow maintenance quiescence stimulus leads to shallow quiescence depth.
(a) Representative images of HUVEC under static (non-flow) or Flow-M (flow maintenance) conditions with EdU incorporation and fixation at indicated times post Flow-M release. Cultures stained for DAPI (white, nuclear mask) and EdU (red, s-phase) or pRB (blue, interphase). Scale bar, 50 µm. White arrow, flow direction. **(b)** Quantification of percent EdU+ cells with indicated conditions. n=3 replicates, 5 images per condition per replicate. **(c)** Quantification of percent pRB+ cells with indicated conditions. n=3 replicates, 5 images per condition per replicate. **(d)** Representative images of HUVEC under low or high density conditions with EdU incorporation and fixation at indicated times post high-density release. Cultures stained for DAPI (white, nuclear mask) and EdU (red, s-phase) or pRB (blue, interphase). Scale bar, 50 µm. **(e)** Quantification of percent EdU+ cells with indicated conditions. n=3 replicates, 6 images per condition per replicate. **(f)** Quantification of percent pRB+ cells with indicated conditions. n=3 replicates, 6 images per condition per replicate. Statistics, one-way ANOVA with Tukey's multiple comparisons test; *$p \leq 0.05$, ** $p \leq 0.01$, *** $p \leq 0.001$, ****$p \leq 0.0001$, *ns = not significant*.

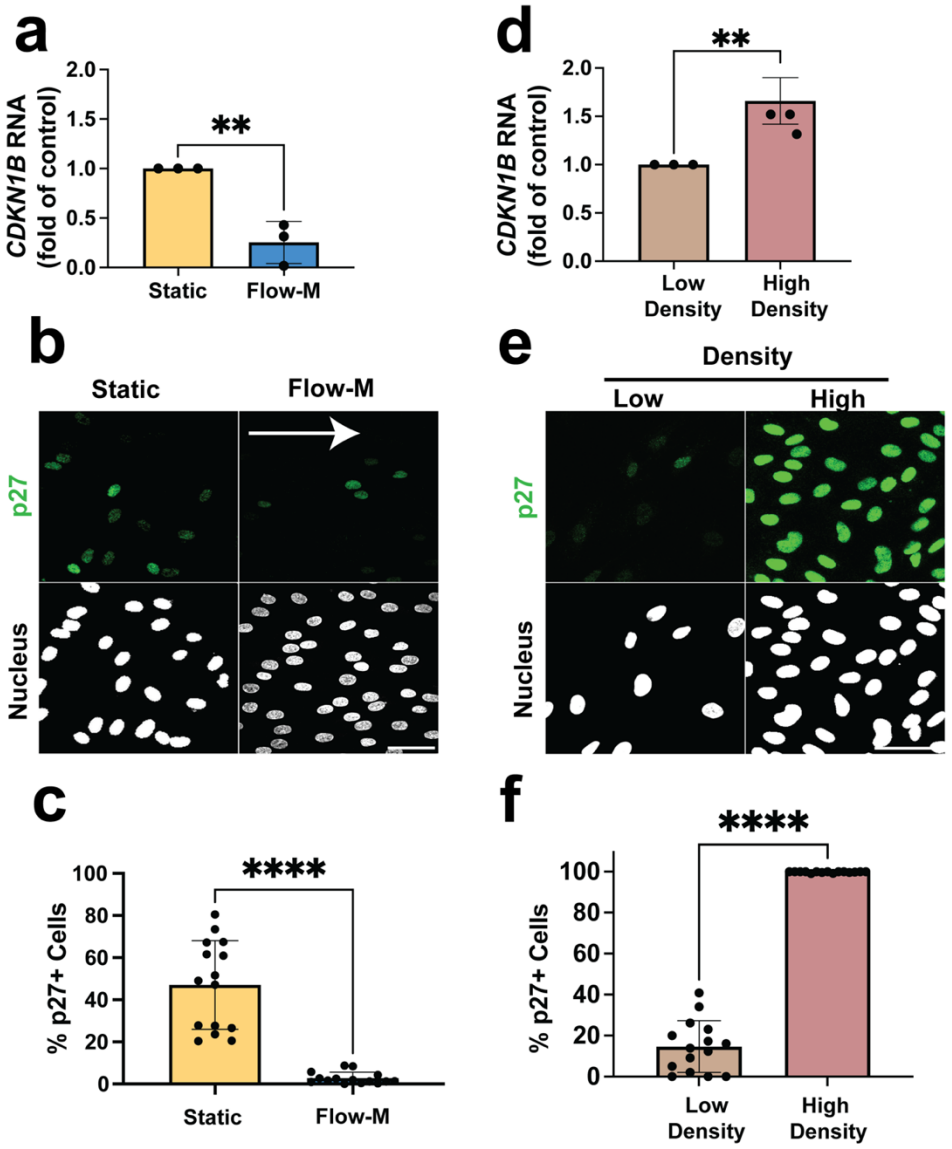

Figure 3. Cell cycle inhibitor p27 expression levels vary with endothelial quiescence stimulus.
(a) RT-qPCR for *CDKN1B* levels in indicated conditions. n=3 replicates. **(b)** Representative images of HUVEC under indicated conditions stained for p27 (green) and DAPI (white, nuclear mask). Scale bar, 50 µm. White arrow, flow direction. **(c)** Quantification of HUVEC p27+ cells under indicated conditions, n=3 replicates, 5 images per condition per replicate. **(d)** RT-qPCR for *CDKN1B* levels in indicated conditions. n=3 replicates. **(e)** Representative images of HUVEC under indicated conditions stained for p27 (green) and DAPI (white, nuclear mask). Scale bar, 50 µm. **(f)** Quantification of HUVEC p27+ cells under indicated conditions. n=3 replicates, 5 images per condition per replicate. Statistics, student's two-tailed *t*-test; ** $p \leq 0.01$, **** $p \leq 0.0001$.

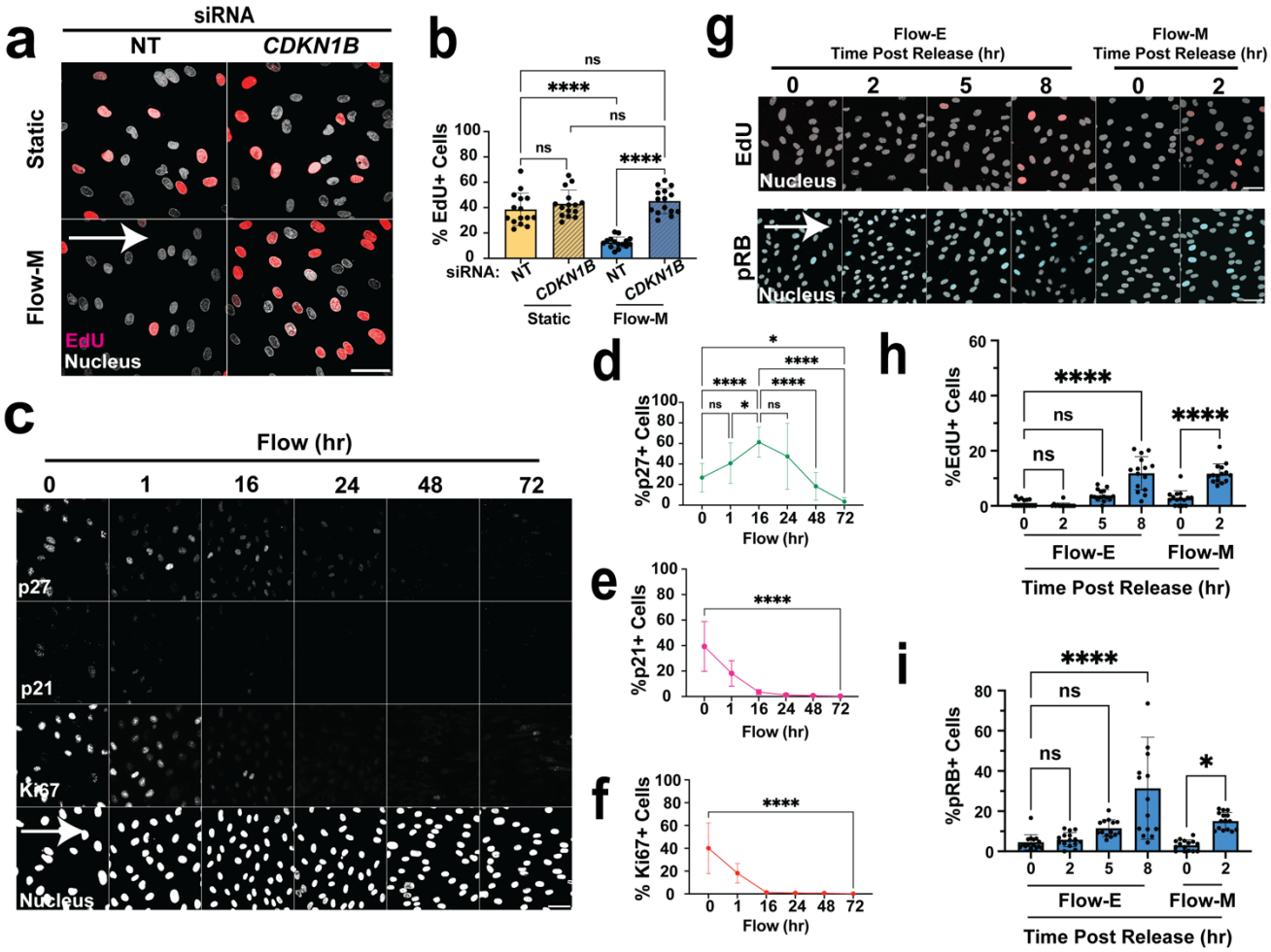

Figure 4. Endothelial quiescence depth varies with laminar flow exposure time and positively correlates with p27 expression levels

(a) Representative images of HUVEC with indicated siRNA treatments and conditions. after EdU incorporation (red, S-phase) and staining with DAPI (white, nuclear mask). Scale bar, 50 µm. White arrow, flow direction. **(b)** Quantification of EdU+ cells with indicated conditions. n=3 replicates, 5 images per condition per replicate. **(c)** Representative images of HUVEC with indicated conditions and stained for p27 (inhibitor), p21 (inhibitor), Ki67 (proliferation marker), and DAPI (nucleus) in white. Scale bar, 50 µm. White arrow, flow direction. **(d-f)** Quantification of percent p27+ (d), p21+ cells (e), or Ki67+ cells (f). n=3 replicates, 5 images per condition per replicate, **(g)** Representative images of HUVEC under indicted conditions and after EdU incorporation (red, S-phase) and stained for pRB (blue, interphase) and with DAPI (white, nuclear mask), Flow-E, flow establishment; Flow-M, flow maintenance. Scale bar, 50 µm. White arrow, flow direction. **(h)** Quantification of EdU+ cells in indicated conditions. n=3 replicates, 5 images per condition per replicate. **(i)** Quantification of pRB+ cells in indicated conditions. n=3 replicates, 5 images per condition per replicate. Statistics, one-way ANOVA with Tukey's multiple comparisons test; *$p \leq 0.05$, ****$p \leq 0.0001$, *ns = not significant*.

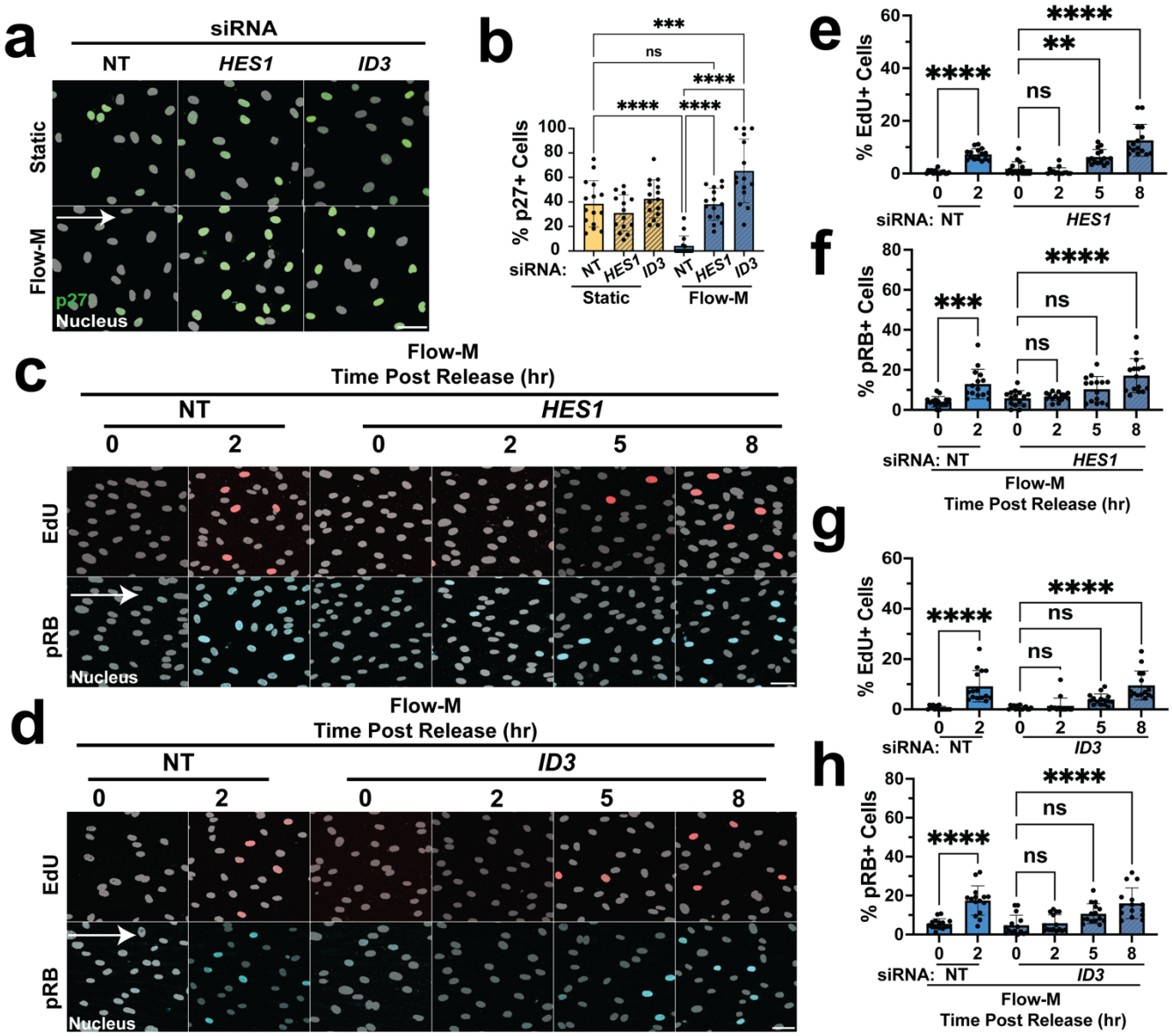
a
siRNA
NT
HES1
ID3
Static
Flow-M
p27
Nucleus
b
% p27+ Cells
siRNA:
NT
HES1
ID3
Static
Flow-M
***
ns
****
c
Flow-M
Time Post Release (hr)
EdU
pRB
Nucleus
d
e
% EdU+ Cells
f
% pRB+ Cells
g
h

1364 **Figure 5. BMP and NOTCH regulated p27 repressors *HES1* and *ID3* regulate p27**
1365 **levels and flow-mediated quiescence depth**
1366 **(a)** Representative images of HUVEC under indicated conditions and with indicated
1367 siRNA treatment. Cells stained for p27 (green) and DAPI (white, nuclear mask). Scale
1368 bar, 50 μm. White arrow, flow direction. **(b)** Quantification of p27+ cells under indicated
1369 conditions and treatments. n=3 replicates, 5 images per condition per replicate. **(c)**
1370 Representative images of HUVEC with indicated conditions and siRNA treatments.
1371 Cells were pulse labeled with EdU (red, S-phase) and stained for pRB (blue, interphase)
1372 and DAPI (white, nuclear mask). Scale bar, 50 μm. White arrow, flow direction. **(d)**
1373 Representative images of HUVEC with indicated conditions and siRNA treatments.
1374 Cells were pulse labeled with EdU (red, S-phase) and stained for pRB (blue, interphase)
1375 and DAPI (white, nuclear mask). Scale bar, 50 μm. White arrow, flow direction. **(e)**
1376 Quantification of EdU+ cells with indicated conditions. n=3 replicates, 5 images per
1377 condition per replicate. **(f)** Quantification of pRB+ cells with indicated conditions. n=3
1378 replicates, 5 images per condition per replicate. **(g)** Quantification of EdU+ cells with
1379 indicated conditions. n=3 replicates, 5 images per condition per replicate. **(h)**
1380 Quantification of pRB+ positive cells with indicated conditions. n=3 replicates, 5 images
1381 per condition per replicate. Statistics, one-way ANOVA with Tukey's multiple
1382 comparisons test. *** $p \leq 0.01$, *** $p \leq 0.001$, ****$p \leq 0.0001$, *ns = not significant*.
1383
1384
1385
1386
1387
1388
1389
1390
1391
1392
1393
1394

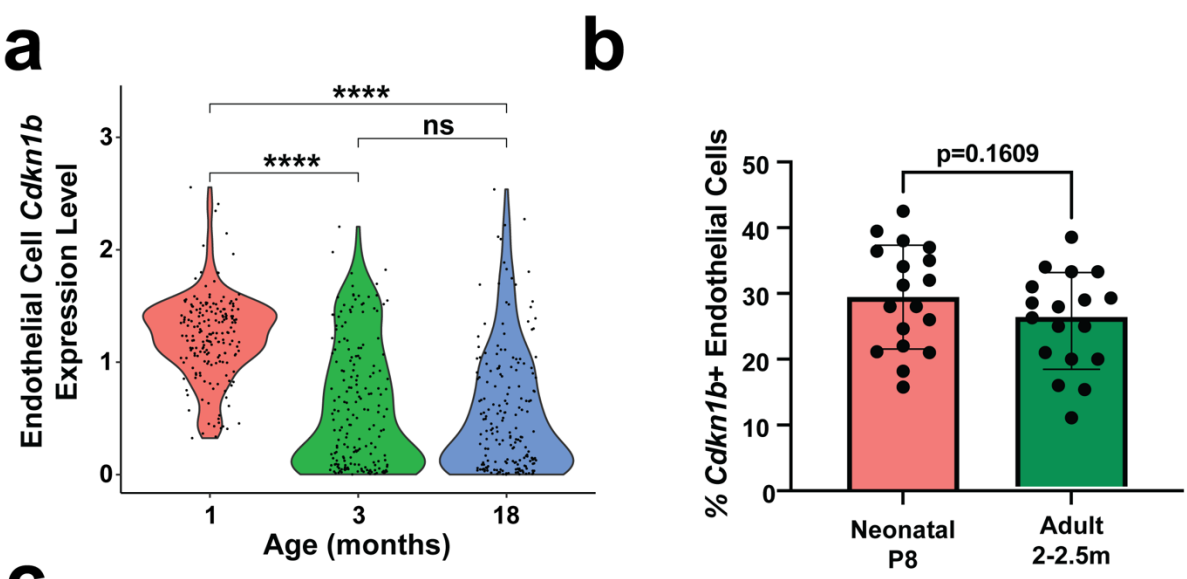
a
Endothelial Cell Cdkn1b Expression Level
****
ns
****
0
1
2
3
1
3
18
Age (months)
b
% Cdkn1b+ Endothelial Cells
p=0.1609
0
10
20
30
40
50
Neonatal P8
Adult 2-2.5m

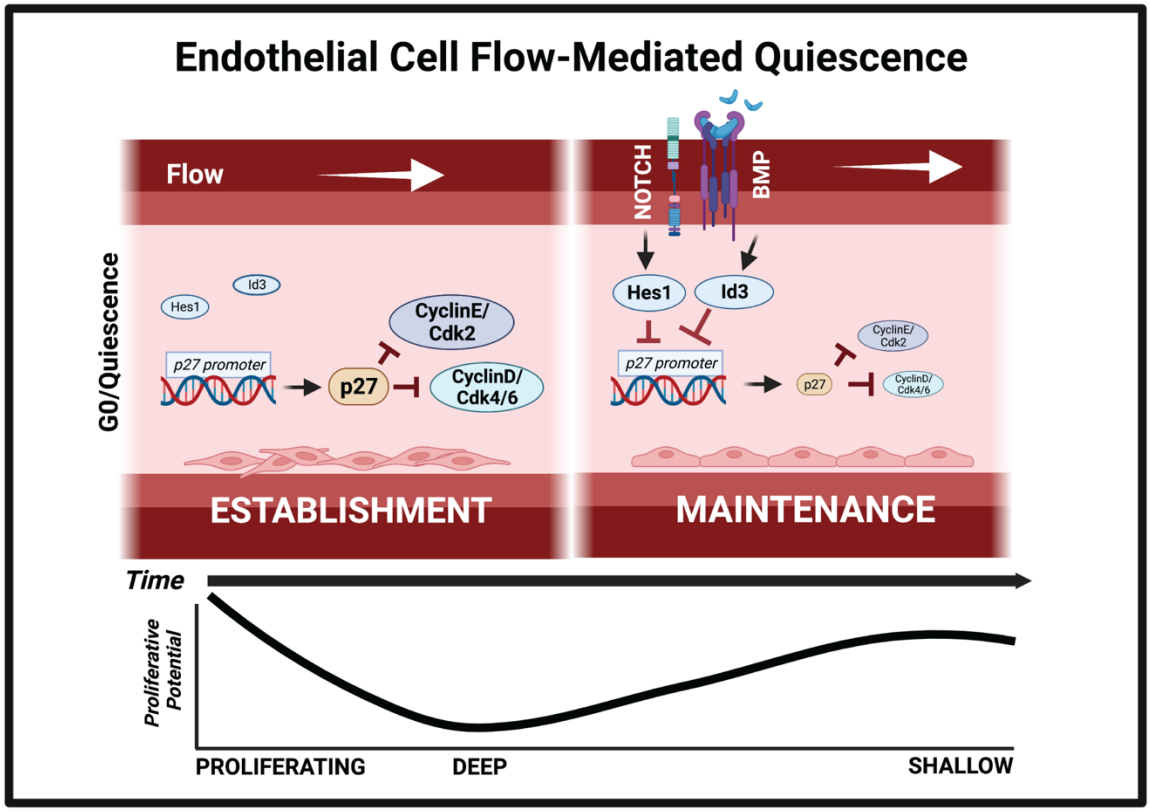
c
Endothelial Cell Flow-Mediated Quiescence
Flow
NOTCH
BMP
G0/Quiescence
Hes1
Id3
CyclinE/ Cdk2
p27 promoter
p27
CyclinD/ Cdk4/6
ESTABLISHMENT
MAINTENANCE
Time
Proliferative Potential
PROLIFERATING
DEEP
SHALLOW

1436 **Figure 6. *Cdkn1b* expression does not accumulate with age *in vivo***
1437 **(a)** scRNAseq analysis of normalized *Cdkn1b* expression in endothelial cells isolated
1438 from mice of indicated ages. See Methods and text for details of dataset reanalysis.
1439 Endothelial cells with *Cdkn1b* expression at 0 were excluded from analysis. ****$p \leq$
1440 *0.0001, ns = not significant* by one-way ANOVA with Tukey's multiple comparisons test.
1441 **(b)** scRNAseq analysis of percent *Cdkn1b*+ endothelial cells isolated from neonatal (P8)
1442 or adult (2-2.5m) murine ears. Each dot represents one endothelial subpopulation in
1443 one sample. Statistics, student's two-tailed *t*-test **(c)** Proposed model for dynamic
1444 regulation of endothelial cell flow-mediated quiescence depth with flow exposure time.
1445 In the first 16-24 hr (Flow-E, flow establishment), a deep quiescence is established
1446 accompanied by high levels of cell cycle inhibitor p27. With time, transcription factors
1447 that are targets of flow-mediated Notch and BMP signaling are upregulated, and these
1448 p27 transcriptional repressors prevent ongoing p27 synthesis and lead to significantly
1449 reduced p27 levels. The regulators are required to transition to a shallow quiescence
1450 depth that characterizes extended exposure to laminar flow (Flow-M, flow
1451 maintenance).
1452